Cage effects control the mechanism of methane hydroxylation in zeolites

Benjamin E. R. Snyder[1,†], Max L. Bols[2,†], Hannah M. Rhoda[1,†], Dieter Plessers[2], Robert A. Schoonheydt[2,*], Bert F. Sels[2,*], and Edward I. Solomon[1,3,*]

Affiliations:
[1]Department of Chemistry, Stanford University, Stanford, California 94305, United States

[2]Department of Microbial and Molecular Systems, Centre for Sustainable Catalysis and Engineering, KU Leuven – University of Leuven, Celestijnenlaan 200F, B-3001 Leuven, Belgium.

[3]Stanford Synchrotron Radiation Lightsource, SLAC National Accelerator Laboratory, Stanford University, Menlo Park, CA 94025

[†]These authors contributed equally to this work.
*Correspondence to: robert.schoonheydt@biw.kuleuven.be; bert.sels@kuleuven.be; edward.solomon@stanford.edu.

Abstract: Catalytic conversion of methane to methanol remains an economically tantalizing but fundamentally challenging goal. Current technologies based on zeolites deactivate too rapidly for practical application. Here, we show similar active sites hosted in different zeolite lattices can exhibit dramatically different reactivity with methane depending on the size of the zeolite pore apertures. Whereas the zeolite with large pore apertures deactivates completely following single turnover, 40% of active sites in the zeolite with small pore apertures are regenerated, enabling a catalytic cycle. Detailed spectroscopic characterization of reaction intermediates together with density functional theory calculations show that hindered diffusion through small pore apertures disfavors premature release of CH_3 radicals from the active site following C-H activation, thereby promoting radical recombination to form methanol rather than deactivated Fe-OCH_3 centers elsewhere in the lattice.

One Sentence Summary: In zeolites, the pore environment of the active site determines whether the active site is deactivated or regenerated following C-H activation of methane.

Main Text: Methane is an abundant source of energy and a potent greenhouse gas. Its direct conversion to methanol under mild conditions remains an economically tantalizing but fundamentally challenging goal of modern chemistry. Iron active sites in zeolites and enzymes have attracted considerable attention based on their capacity to hydroxylate the otherwise largely inert (104 kcal/mol) C-H bond of methane rapidly at room temperature.(*1–5*) In iron-containing zeolites (Fe-zeolites), prior studies suggest this reaction occurs at a mononuclear square pyramidal high-spin (S=2) Fe(IV)=O intermediate (α-Fe(IV)=O) that is activated for H-atom abstraction by a constrained coordination geometry enforced by the zeolite lattice.(*6–9*) α-Fe(IV)=O is generated *via* O-atom transfer from N_2O to an S=2 square planar Fe(II) precursor, α-Fe(II). At low temperature (<200 °C), α-Fe(IV)=O reacts in a non-catalytic fashion with CH_4.(*10*) Catalytic oxidation of CH_4 is proposed to occur at higher temperatures, but with poor selectivity (<10%) for methanol, and on undefined active sites.(*10*, *11*) The absence of a closed catalytic cycle for selective methanol synthesis represents a critical barrier to scale-up.(*4*) Mechanistic insight into catalyst deactivation is limited and, despite intensive effort, no strategy or design principle has emerged to mediate this challenge. In nature, many metalloenzymes – including soluble methane monooxygenase (sMMO)(*3*, *5*, *12*) – have evolved active site pockets that exert precise control over hydrocarbon substrate radicals, shutting down deactivating mechanisms involving radical escape, and instead guiding radical recombination to selectively form R-OH or R-X bonds.(*3*, *12–14*) Translating the active site pocket concept to small molecules(*15–18*) and microporous materials(*19–23*) is an appealing strategy to improve catalysis. Zeolite micropore effects have been shown (or proposed) to tune reactivity and/or selectivity across a number of model reactions.(*9*, *20*, *24–27*) However, micropore effects enabling precise control over the fate of small reactive intermediates, as with the active site

pocket of sMMO, remain elusive. Here, we demonstrate that steric effects from a constricted pore aperture act as a cage, controlling the extremely reactive methyl radical generated by methane C-H activation. A radical recombination pathway for direct methanol synthesis analogous to the sMMO pathway can then ensue.

While evaluating Fe active sites in a number of zeolites lattices, we discovered a dramatic difference in the methane reactivity of α-Fe(IV)=O sites stabilized in zeolite beta (*BEA)(*6*, *7*) and chabazite (CHA).(*8*) These active sites have highly similar first coordination spheres (Fig. 1A), as reflected in their ^{57}Fe Mössbauer spectra, which nearly overlay (Fig. 2A).(*7*, *8*) However, there are differences in the local pore environments of these active sites (Fig. 1B). In *BEA, α-Fe(IV)=O is accessed through large channels defined by 12-membered rings of SiO_4 tetrahedra. In CHA, α-Fe(IV)=O is located in a cage-like pore environment. Though the dimensions of the CHA cage are similar to the *BEA pore, substrates must pass through a constricted 8-membered ring aperture to enter the cage. (*7*, *8*, *28*) The maximum van der Waals diameter of a molecule that can freely diffuse out of this constricted aperture is 3.7 Å, *versus* 5.9 Å for *BEA (fig. 1B). As the van der Waals diameter of CH_4 is larger than 3.7 Å (4.1-4.2 Å(*29*)), diffusion of substrate through the pore aperture to/from the active site should be hindered in CHA, but not *BEA.

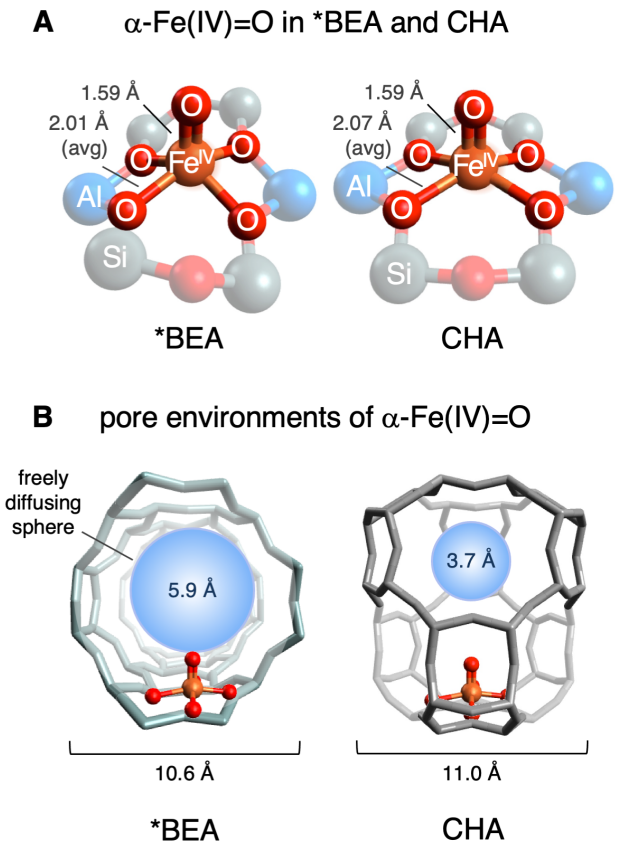

Figure 1. Local environments of α-Fe(IV)=O sites in *BEA and CHA. (A) Comparison of first coordination spheres, with bond lengths from spectroscopically-calibrated DFT models.(*6–8*) **(B)** Comparison of α-Fe(IV)=O pore environments in *BEA (left) and CHA (right). For each lattice, a freely diffusing sphere of maximal size is included for reference.

We exposed α-Fe(IV)=O active sites in compositionally similar *BEA (Si/Al=12.3, 0.30 wt.% Fe) and CHA (Si/Al=8.9, 0.24 wt.% Fe) to 1 atm of methane at room temperature, and used Mössbauer spectroscopy to track the state of the iron active sites under single turnover conditions. The low iron loadings used in these samples exclude the presence of multiple Fe active sites in a single CHA cage. From data presented in Fig. 2B, there is a remarkable difference in the state of the iron active sites in the post-reaction materials. In *BEA (red trace), a broad distribution of spectral intensity is observed, reflecting the dominant contributions from deactivated, partially oxidized active sites (see below and Fig. S1 for assignments). In this lattice, only a small fraction α-Fe(II) is regenerated (ca. 4%). In contrast, for CHA (Fig. 2B, black trace), a significant fraction of α-Fe(II) is regenerated (37±5% yield based on α-

Fe(IV)=O), potentially enabling further turnover. To evaluate this possibility, we performed reactivity studies including a second reaction cycle. Samples of Fe-*BEA (Si/Al=9.4, 0.26 wt.% Fe) and Fe-CHA (Si/Al=8.9, 0.24 wt.% Fe) were subjected to either one or two cycles of N_2O activation and room temperature CH_4 reaction, and then products were desorbed and quantified by on-stream mass spectrometry. (We note this method results in a modest systematic underestimate of MeOH yields – see SI methods for details.) To parse the desorbed methanol into contributions from different reaction cycles, $^{13}CH_4$ was used for the first reaction cycle, and $^{12}CH_4$ was used for the second (see figure 2C and methods). These reactions were also monitored by Mössbauer spectroscopy (see figure S2). The one-cycle yield of CHA (0.33±0.03 MeOH/Fe) is similar to that of BEA (0.27±0.03 MeOH/Fe). However, after accounting for the different α-Fe(IV)=O concentrations of the samples used for these reactivity studies (74±5% of Fe for CHA, 91±5% for BEA – see figure S2), the one-cycle yield of CHA is found to be 50±25% greater than that of BEA. A more significant difference is observed in the two cycle yields. For BEA, very little $^{12}CH_3OH$ is generated during the second reaction cycle, and the total yield of the two-cycle reaction is the same (within error) as the one-cycle reaction. This is consistent with the nearly complete deactivation of BEA observed by Mössbauer spectroscopy following single turnover (figure 2B). For CHA, a significant amount of $^{12}CH_3OH$ is generated during the second reaction cycle, and as a result, the total yield of the two-cycle reaction is 40±20% higher than that of the one-cycle reaction. This correlates well to the 37±5% regeneration of α-Fe(II) observed by Mössbauer spectroscopy (figure 2B). Finally, accounting for the different α-Fe(IV)=O concentrations of these CHA and BEA samples, the two-cycle yield of α-Fe(IV)=O in CHA is approximately twice that of *BEA.

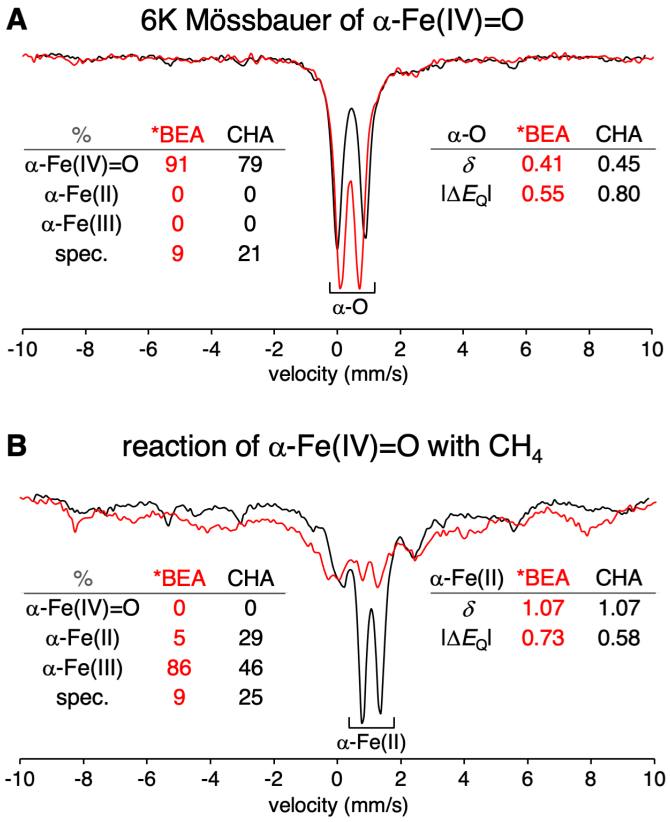

C catalyst cycling studies

methanol yields		$^{13}CH_3OH$/Fe	$^{12}CH_3OH$/Fe	total/Fe	total/α-O
*BEA	one cycle	0.25 ± 0.02	0.02 ± 0.02	0.27 ± 0.03	0.30 ± 0.04
	two cycle	0.24 ± 0.02	0.04 ± 0.02	0.28 ± 0.03	0.31 ± 0.04
CHA	one cycle	0.30 ± 0.02	0.03 ± 0.02	0.33 ± 0.03	0.45 ± 0.05
	two cycle	0.26 ± 0.02	0.21 ± 0.02	0.47 ± 0.03	0.64 ± 0.06

Figure 2. Effect of lattice topology on active site regeneration. (A) Normalized 6K Mössbauer spectra of N_2O-activated Fe-*BEA (red) and Fe-CHA (black). Spectral contributions from each Fe oxidation state are quantified at the left (spec. = spectator components that do not contribute to reactivity). Parameters of the α-Fe(IV)=O components are indicated at the right. **(B)** Normalized Mössbauer spectra of N_2O-activated Fe-*BEA (red) and Fe-CHA (black) reacted with CH_4 at 300 K, and then cooled to 6K for data collection. Spectral contributions from each oxidation state of the active site are quantified at the left. Parameters of the α-Fe(II) components are indicated at the right. See Fig. S1 for detail on quantification. The given quantifications have an error of ±5%. δ = isomer shift, ΔE_Q = quadrupole splitting (values given in mm/s). **(C)** Comparison of methanol yields extracted following one reaction cycle with $^{13}CH_4$ versus two cycles ($^{13}CH_4$, then $^{12}CH_4$). Yields based on initial α-Fe(IV)=O content make use of Mössbauer quantifications presented in figure S2.

To understand the mechanistic origin of the differences in reactivity between CHA and *BEA, we performed additional spectroscopic experiments to characterize the Fe(III) components present in Fe-*BEA after reaction with CH_4, where only 4% of the α-Fe(II) active site is regenerated. The reaction of H_2 with α-Fe(IV)=O in *BEA was first studied as a reference, as we anticipated this would form a single Fe(III) species: the α-Fe(III)-OH product of H-atom transfer to α-Fe(IV)=O. From Mössbauer spectroscopy, this reaction generates a new majority component that exhibits hyperfine structure in the absence of an external magnetic field (Fig. 3a, filled blue trace). The signature is consistent with a mononuclear S=5/2 Fe(III) center with a small zero-field splitting (quadrupole splitting ΔE_Q=-1.6±0.1 mm/s, isomer shift δ=0.5±0.1 mm/s, axial zero field splitting $|D|$=0.3±0.2 cm^{-1}, rhombicity E/D=0.25±0.05 - see methods for detail). The high population of this component (61% of Fe) indicates that it originated from α-Fe(IV)=O (initially 74% of total Fe; ~80% of α-Fe(IV)=O was converted to this Fe(III) product – see Fig. S1). A quadrupole doublet with an isomer shift and quadrupole splitting identical to α-Fe(III)-OH was also generated (17% of Fe, Fig. 3a, purple trace). Based on correlation to post-CH_4 reaction samples (*vide infra*), we assign this band to a rapidly relaxing α-Fe(III)-OH site (α-Fe(III)-OH').

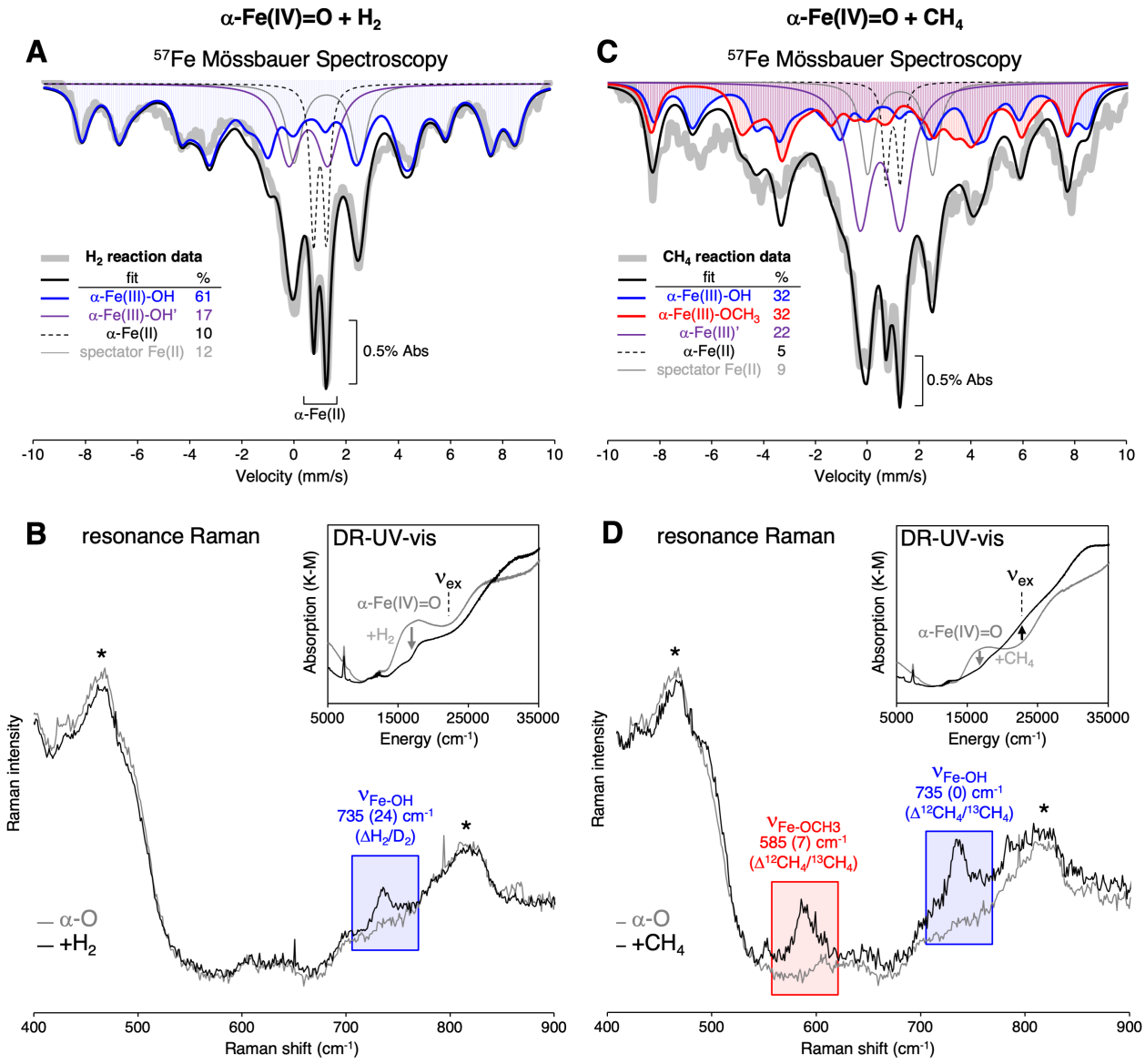

Figure 3. Identification of Fe(III) species after H_2 and CH_4 reactions with Fe-*BEA. (A) 6K ^{57}Fe Mössbauer after H_2 reaction with Fe-*BEA: the Mössbauer signal from the α-Fe(III)-OH product of H-atom transfer to α-Fe(IV)=O is shown in the blue solid trace; **(B)** rR (ν_{ex}=21800 cm^{-1}) of α-Fe(IV)=O before (gray trace) and after (black trace) reaction with H_2 in the Fe-*BEA lattice, DR-UV-vis before (gray trace) and after (black trace) the reaction is shown in the inset. Peaks marked with '*' are (non-resonant) Raman vibrations of the zeolite lattice. **(c)** 6K ^{57}Fe Mössbauer after CH_4 reaction with Fe-*BEA. The Mössbauer signal from α-Fe(III)-OH is shown in the filled blue trace, and the Mössbauer signal for α-Fe(III)-OCH_3 is shown in the filled red trace. **(d)** rR (ν_{ex}=21800 cm^{-1}) of α-Fe(IV)=O before (gray trace) and after (black trace) reaction with CH_4 in the Fe-*BEA lattice, DR-UV-vis before (gray trace) and after (black trace) the reaction is shown in the inset.

Resonance Raman (rR) experiments were performed to further characterize the structure of this majority Fe(III) product. As shown in the inset for the H_2 reaction in Fig. 3b, the reaction of α-Fe(IV)=O with H_2 in *BEA results in a change in the absorption spectrum, including the loss of the characteristic 16900 cm^{-1} Abs feature of α-Fe(IV)=O (gray trace). Tuning a laser to the 22000 cm^{-1} shoulder of the resonance of the sample after H_2 reaction enhances a single Raman vibration at 735 cm^{-1} (Fig. 3b, blue highlight; see Fig. S3a for rR profile). This vibration shifts down by 24 cm^{-1} using D_2 as the substrate (see Fig. S3b). The frequency and isotope sensitivity of the 735 cm^{-1} vibration are consistent with the stretching mode of a terminal Fe(III)-OH bond,(*30*) and we assign this band to the α-Fe(III)-OH product of H-atom abstraction from H_2. The experimentally defined spectroscopic features of α-Fe(III)-OH are reproduced by DFT calculations presented in Fig. S4a.

Next, we considered the reaction of α-Fe(IV)=O with CH_4 in *BEA. As shown in the inset in Fig. 3d, the 16900 cm^{-1} DR-UV-vis band of α-Fe(IV)=O (gray trace) is eliminated upon reaction with CH_4, and new intensity grows in at ~22000 cm^{-1} (black trace). Tuning a laser to this absorption resonance enhances a 735 cm^{-1} vibration assigned to α-Fe(III)-OH (from correlation to the above results from the H_2 reaction), along with an additional vibration at 585 cm^{-1} (Fig. 3d, red highlight – see rR profile in Fig. S3). Unlike the 735 cm^{-1} band, this mode shows a $^{12}C/^{13}C$ isotope sensitivity ($\Delta^{12}CH_4/^{13}CH_4$= 7 cm^{-1} – see Fig. S3). It therefore involves motion of a methane-derived ligand. Its frequency and isotope sensitivity are consistent with the stretching mode of an Fe(III)-OCH_3 species. This observation indicates that free methyl radicals generated during C-H activation of CH_4 in *BEA go on to recombine with remote α-Fe(IV)=O sites to form deactivated α-Fe(III)-OCH_3 species. This is consistent with previous identification of -OH and -CH_3 fragments in Fe-zeolites that have reacted with methane(*31*, *32*); however these

fragments were not shown to be related to the iron active sites. The experimentally defined spectroscopic features of α-Fe(III)-OCH_3 are reproduced by DFT calculations presented in Fig. S4b.

For the reaction of α-Fe(IV)=O in Fe-*BEA with CH_4 (Fig. 3C), hyperfine features are also observed by Mössbauer spectroscopy, but with a different intensity distribution relative to the sample that reacted with H_2. This observation parallels the rR data, showing that two Fe(III) species are present following the CH_4 reaction: α-Fe(III)-OH and α-Fe(III)-OCH_3. Fitting the broad distribution of Fe(III) hyperfine intensity in the Mössbauer spectrum (Fig. 3C) requires a contribution from α-Fe(III)-OH (filled blue trace), as well as a second hyperfine-split component that we assign as α-Fe(III)-OCH_3 (filled red trace). The parameters of α-Fe(III)-OCH_3 are similar to those of α-Fe(III)-OH, but with a smaller E/D (ΔE_Q= -1.6±0.1 mm/s, δ=0.5±0.1 mm/, $|D|$=0.3±0.2 cm^{-1}, E/D=0.15±0.05 - see methods). The α-Fe(III)-OH and α-Fe(III)-OCH_3 components are present in equal amounts (each 32% of Fe). In addition, a quadrupole doublet representing 22% of Fe and identical to that identified in the H_2 reaction appears (purple trace in Fig. 3C). Given the initial 91% of Fe as α-Fe(IV)=O, this 22% component must derive from α-Fe(IV)=O. Likely the doublet represents rapid relaxation of α-Fe(III)' sites, encompassing both α-Fe(III)-OH and α-Fe(III)-OCH_3, leading to both a hyperfine component and a doublet component in their Mössbauer spectra. Together, the α-Fe(III) components sum to 86±9% of Fe in the sample – within error of the 91±5% of α-Fe(IV)=O initially present.

Mössbauer and rR data from Fe-*BEA therefore reflect the near-quantitative conversion of α-Fe(IV)=O to a 1:1 mixture of α-Fe(III)-OCH_3 and α-Fe(III)-OH following single turnover. Parallel spectroscopic data from α-Fe(IV)=O in CHA after reaction with CH_4 show α-Fe(III)-OCH_3 and α-Fe(III)-OH sites do form in this lattice following CH_4 reaction, but in much lower

concentrations relative to *BEA: only ~60% of the total α-Fe(IV)=O in CHA reacts with CH_4 to form α-Fe(III)-OCH_3/α-Fe(III)-OH (see S1 and S5), with the remaining ~40% regenerating α-Fe(II). As one radical escape event produces two Fe(III) centers (one equivalent each of α-Fe(III)-OH and α-Fe(III)-OCH_3), rebound is favored over cage escape by a ratio of ~4:3 in CHA at room temperature. This model yields two key predictions: i) the single-cycle yield of CHA should be ~40% greater than that of *BEA, and ii) the two-cycle yield of CHA should be ~40% greater than the one-cycle yield. Both predictions are borne out in the MeOH yields tabulated in figure 2C, further supporting the model of competing cage escape and radical rebound mechanisms.

Mössbauer and rR data show the similar α-Fe(IV)=O sites in CHA and *BEA give different Fe products following their single turnover reaction with methane. In *BEA, exclusively deactivated Fe(III) species are observed, whereas in CHA, a significant fraction of the active sites is returned to the reduced, catalytically active Fe(II) state. We were interested to correlate this difference in reactivity to the structures of the *BEA and CHA lattices. As the van der Waals diameter of CH_4 is larger than the 3.7 Å pore aperture of CHA,(*29*) we performed density functional theory (DFT) calculations to evaluate whether the small pore of CHA gates methyl radical escape from the active site (Fig. 4, right path), thus enhancing methanol synthesis through direct radical rebound on the active site (Fig. 4, left path). Cage escape in *BEA and CHA was modeled *via* passage of CH_3 through a 12MR and an 8MR, respectively (the rings gating egress from the active site in each zeolite). Proceeding from spectroscopically validated models of α-Fe(III)-OH (see Fig. S4A) in a van der Waals complex with CH_3 (Fig. 4, center), our calculations indicate a striking difference between the cage escape pathways for *BEA and CHA (Fig. 4, right path). For the large 12MR channel of *BEA, there is no barrier to CH_3 radical

escape (see red inset of Fig. 4). The liberated CH_3 radical is then free to react with a remote α-Fe(IV)=O center, forming α-Fe(III)-OCH_3 and leaving behind one equivalent of α-Fe(III)-OH (as observed experimentally in Fig. 3). This reaction is calculated to be highly exergonic (ΔG=-85 kcal/mol), proceeding without an activation barrier. The absence of a rate-limiting barrier for cage escape explains the experimental observation of exclusively ferric products in *BEA. For CHA, on the other hand, there is an activation barrier of 5.2 kcal/mol for CH_3 escape (TS1) through the constricted 8MR pore of the CHA cage (see Fig. 4, inset). Based on the experimentally determined 3:4 branching ratio for cage escape *versus* radical recombination, this activation barrier is likely overestimated.

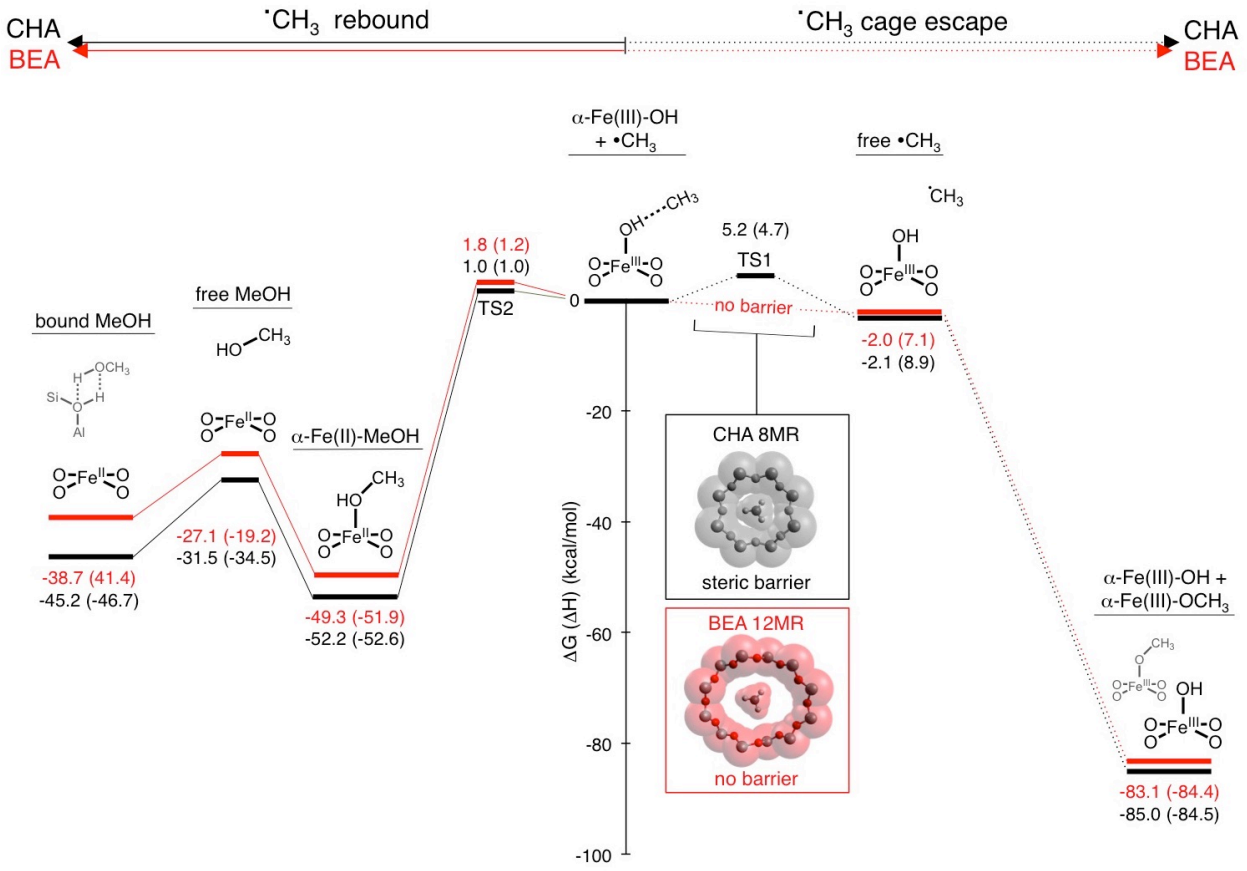

Figure 4. Comparison of post H-atom abstraction reaction coordinates for *BEA (red) and CHA (black). The reaction coordinates for radical rebound (left) and cage escape (right) are presented. Free energy changes (ΔG at 300K, ΔH in parentheses) are given relative to the α-Fe(III)-OH···CH_3 van der Waals complex produced during H-atom abstraction from CH_4 by α-Fe(IV)=O. The inset compares the van der Waals surfaces of an 8MR of CHA to a 12MR of *BEA, illustrating how the constricted CHA 8MR creates a steric barrier for radical escape from the CHA active site (TS1).

Although the cage escape pathways for *BEA and CHA differ, their radical rebound mechanisms are similar (Fig 4. left path): in both cases, radical rebound proceeds with a low barrier (TS2, $\Delta G^{\ddagger}$=1-2 kcal/mol) and is highly exergonic, forming methanol-ligated α-Fe(II) (α-Fe(II)-CH_3OH). The ~50 kcal/mol of free energy released in this reaction would drive desorption of MeOH into the gas phase, where it is modeled to bind to the Brønsted acid sites

present in large excess in this zeolite lattice. This regenerates α-Fe(II), as observed experimentally in CHA, but not *BEA (Fig. 2B).

Thus in *BEA (and other zeolites with large pore apertures), escape of a CH_3 radical from the α-Fe(III)-OH intermediate is expected to be a diffusive process, leading to catalytically inactivated Fe(III) products (α-Fe(III)-OCH_3/α-Fe(III)-OH). Steaming is required to recover MeOH *via* hydrolysis of α-Fe(III)-OCH_3, and high temperatures must then be used to effect autoreduction of the resulting Fe(III) sites back to α-Fe(II).(*33*) In contrast, the constricted pore apertures of CHA constrain the CH_3 radical, promoting its recombination with α-Fe(III)-OH to form CH_3OH, returning the active site to its reduced α-Fe(II) state to enable further turnover. In analogy to the active site pocket of a metalloenzyme, the local pore environment of a heterogeneous active site can therefore play a decisive role in selecting between competing reaction pathways with low activation barriers, in this case promoting selective hydroxylation and precluding deactivating side reactions. This strategy is potentially broadly applicable for synthetic control over catalytic mechanisms in microporous materials.

References

1. G. I. Panov, V. I. Sobolev, A. S. Kharitonov, The role of iron in N2O decomposition on ZSM-5 zeolite and reactivity of the surface oxygen formed. *J. Mol. Catal.* **61**, 85–97 (1990).
2. K. A. Dubkov, V. I. Sobolev, G. I. Panov, Low-temperature oxidation of methane to methanol on FeZSM-5 zeolite. *Kinet. Catal.* **39**, 72–79 (1998).
3. M. O. Ross, A. C. Rosenzweig, A tale of two methane monooxygenases. *J. Biol. Inorg. Chem.* **22**, 307–319 (2017).

4. B. E. R. Snyder, M. L. Bols, R. A. Schoonheydt, B. F. Sels, E. I. Solomon, Iron and Copper Active Sites in Zeolites and Their Correlation to Metalloenzymes. *Chem. Rev.* **118**, 2718–2768 (2018).

5. R. Banerjee, Y. Proshlyakov, J. D. Lipscomb, D. A. Proshlyakov, Structure of the key species in the enzymatic oxidation of methane to methanol. *Nature*. **518**, 431–434 (2015).

6. B. E. R. Snyder, P. Vanelderen, M. L. Bols, S. D. Hallaert, L. H. Böttger, L. Ungur, K. Pierloot, R. A. Schoonheydt, B. F. Sels, E. I. Solomon, The active site of low-temperature methane hydroxylation in iron-containing zeolites. *Nature*. **536**, 317–321 (2016).

7. B. E. R. Snyder, L. H. Böttger, M. L. Bols, J. J. Yan, H. M. Rhoda, A. B. Jacobs, M. Y. Hu, J. Zhao, E. E. Alp, B. Hedman, K. O. Hodgson, R. A. Schoonheydt, B. F. Sels, E. I. Solomon, Structural characterization of a non-heme iron active site in zeolites that hydroxylates methane. *Proc. Natl. Acad. Sci.* **115**, 4565–4570 (2018).

8. M. L. Bols, S. D. Hallaert, B. E. R. Snyder, J. Devos, D. Plessers, H. M. Rhoda, M. Dusselier, R. A. Schoonheydt, K. Pierloot, E. I. Solomon, B. F. Sels, Spectroscopic Identification of the α-Fe/α-O Active Site in Fe-CHA Zeolite for the Low-Temperature Activation of the Methane C-H Bond. *J. Am. Chem. Soc.* **140**, 12021–12032 (2018).

9. B. E. R. Snyder, M. L. Bols, H. M. Rhoda, P. Vanelderen, L. H. Böttger, A. Braun, J. J. Yan, R. G. Hadt, J. T. Babicz, M. Y. Hu, J. Zhao, E. E. Alp, B. Hedman, K. O. Hodgson, R. A. Schoonheydt, B. F. Sels, E. I. Solomon, Mechanism of selective benzene hydroxylation catalyzed by iron-containing zeolites. *Proc. Natl. Acad. Sci.* **115**, 12124–12129 (2018).

10. M. V. Parfenov, E. V. Starokon, L. V. Pirutko, G. I. Panov, Quasicatalytic and catalytic oxidation of methane to methanol by nitrous oxide over FeZSM-5 zeolite. *J. Catal.* **318**,

14–21 (2014).

11. B. R. Wood, J. A. Reimer, A. T. Bell, M. T. Janicke, K. C. Ott, Nitrous oxide decomposition and surface oxygen formation on Fe-ZSM-5. *J. Catal.* **224**, 148–155 (2004).

12. X. Huang, J. T. Groves, Beyond ferryl-mediated hydroxylation: 40 years of the rebound mechanism and C–H activation. *JBIC J. Biol. Inorg. Chem.* **22**, 185–207 (2017).

13. M. Srnec, E. I. Solomon, Frontier Molecular Orbital Contributions to Chlorination versus Hydroxylation Selectivity in the Non-Heme Iron Halogenase SyrB2. *J. Am. Chem. Soc.* **139**, 2396–2407 (2017).

14. M. L. Neidig, A. Decker, O. W. Choroba, F. Huang, M. Kavana, G. R. Moran, J. B. Spencer, E. I. Solomon, Spectroscopic and electronic structure studies of aromatic electrophilic attack and hydrogen-atom abstraction by non-heme iron enzymes. *Proc. Natl. Acad. Sci.* **103**, 12966–12973 (2006).

15. H. M. Key, P. Dydio, D. S. Clark, J. F. Hartwig, Abiological catalysis by artificial haem proteins containing noble metals in place of iron. *Nature*. **534**, 534 (2016).

16. R. L. Shook, A. S. Borovik, Role of the Secondary Coordination Sphere in Metal-Mediated Dioxygen Activation. *Inorg. Chem.* **49**, 3646–3660 (2010).

17. J. P. Collman, R. Boulatov, C. J. Sunderland, L. Fu, Functional Analogues of Cytochrome c Oxidase, Myoglobin, and Hemoglobin. *Chem. Rev.* **104**, 561–588 (2004).

18. D. Fiedler, D. H. Leung, R. G. Bergman, K. N. Raymond, Selective Molecular Recognition, C−H Bond Activation, and Catalysis in Nanoscale Reaction Vessels. *Acc. Chem. Res.* **38**, 349–358 (2005).

19. P. Vanelderen, B. E. R. Snyder, M.-L. Tsai, R. G. Hadt, J. Vancauwenbergh, O. Coussens,

R. A. Schoonheydt, B. F. Sels, E. I. Solomon, Spectroscopic Definition of the Copper Active Sites in Mordenite: Selective Methane Oxidation. *J. Am. Chem. Soc.* **137**, 6383–6392 (2015).

20. B. E. R. Snyder, P. Vanelderen, R. A. Schoonheydt, B. F. Sels, E. I. Solomon, Second-Sphere Effects on Methane Hydroxylation in Cu-Zeolites. *J. Am. Chem. Soc.* **140**, 9236–9243 (2018).

21. D. J. Xiao, J. Oktawiec, P. J. Milner, J. R. Long, Pore Environment Effects on Catalytic Cyclohexane Oxidation in Expanded Fe2 (dobdc) Analogues. *J. Am. Chem. Soc.* **138**, 14371–14379 (2016).

22. E. G. Derouane, Shape selectivity in catalysis by zeolites: The nest effect. *J. Catal.* **100**, 541–544 (1986).

23. B. Chen, S. Xiang, G. Qian, Metal−Organic Frameworks with Functional Pores for Recognition of Small Molecules. *Acc. Chem. Res.* **43**, 1115–1124 (2010).

24. F. Göltl, C. Michel, P. C. Andrikopoulos, A. M. Love, J. Hafner, I. Hermans, P. Sautet, Computationally Exploring Confinement Effects in the Methane-to-Methanol Conversion Over Iron-Oxo Centers in Zeolites. *ACS Catal.* **6**, 8404–8409 (2016).

25. M. H. Mahyuddin, A. Staykov, Y. Shiota, M. Miyanishi, K. Yoshizawa, Roles of Zeolite Confinement and Cu–O–Cu Angle on the Direct Conversion of Methane to Methanol by [Cu 2 (μ-O)] 2+ -Exchanged AEI, CHA, AFX, and MFI Zeolites. *ACS Catal.* **7**, 3741–3751 (2017).

26. J. F. Haw, W. Song, D. M. Marcus, J. B. Nicholas, The mechanism of methanol to hydrocarbon catalysis. *Acc. Chem. Res.* **36**, 317–326 (2003).

27. S. M. Csicsery, Shape-selective catalysis in zeolites. *Zeolites*. **4**, 202–213 (1984).

28. J. M. Newsam, M. M. Treacy, W. T. Koetsier, C. B. De Gruyter, Structural characterization of zeolite beta. *Proc. R. Soc. London A Math. Phys. Eng. Sci.* **420**, 375–405 (1988).

29. C. W. Kammeyer, D. R. Whitman, Quantum mechanical calculation of molecular radii. I. Hydrides of elements of periodic groups IV through VII. *J. Chem. Phys.* **56**, 4419–4421 (1972).

30. M. T. Green, Application of Badger's rule to heme and non-heme iron-oxygen bonds: An examination of ferryl protonation states. *J. Am. Chem. Soc.* **128**, 1902–1906 (2006).

31. E. V Starokon, M. V Parfenov, S. S. Arzumanov, L. V Pirutko, A. G. Stepanov, G. I. Panov, Oxidation of methane to methanol on the surface of FeZSM-5 zeolite. *J. Catal.* **300**, 47–54 (2013).

32. G. I. Panov, K. A. Dubkov, Y. A. Paukshtis, in *Catalysis by Unique Metal Ion Structures in Solid Matrices: From Science to Application*, G. Centi, B. Wichterlová, A. T. Bell, Eds. (Springer Netherlands, Dordrecht, 2001), pp. 149–163.

33. G. I. Panov, E. V. Starokon, L. V. Pirutko, E. A. Paukshtis, V. N. Parmon, New reaction of anion radicals O- with water on the surface of FeZSM-5. *J. Catal.* **254**, 110–120 (2008).

34. Schmidt, J. E.; Deimund, M. A.; Xie, D.; Davis, M. E. Synthesis of RTH-Type Zeolites Using a Diverse Library of Imidazolium Cations. *Chem. Mater.* **27**, 3756–3762 (2015).

35. Hallaert, S. D.; Bols, M. L.; Vanelderen, P.; Schoonheydt, R. A.; Sels, B. F.; Pierloot, K. Identification of α-Fe in High-Silica Zeolites on the Basis of Ab Initio Electronic Structure Calculations. *Inorg. Chem.* **56**, 10681–10690 (2017).

36. Frisch, M. J.; Trucks, G. W.; Schlegel, H. B.; Scuseria, G. E.; Robb, M. A.; Cheeseman, J.

R.; Scalmani, G.; Barone, V.; Mennucci, B.; Petersson, G. A.; et al. Gaussian09. Gaussian, Inc.: Wallingford, CT 2009.

37. Baerlocher, C.; McCusker, L. B. http://www.iza-structure.org/databases/ (accessed Feb 4, 2018).

38. Grimme, S.; Antony, J.; Ehrlich, S.; Krieg, H. A Consistent and Accurate Ab Initio Parametrization of Density Functional Dispersion Correction (DFT-D) for the 94 Elements H-Pu. *J. Chem. Phys.* **132**, 154104 (2010).

39. Snyder, B.; Bols, M.; Rhoda, H.; Plessers, D.; Schoonheydt, R.; Sels, B.; Solomon, E. Raw spectroscopic data for "Cage effects control the mechanism of methane hydroxylation in zeolites". Zenodo (2021), doi: 10.5281/zenodo.4735834.

Acknowledgements**:** B.E.R.S. acknowledges support from the National Science Foundation Graduate Research Fellowship Program under grant DGE-11474, and from the Munger, Pollock, Reynolds, Robinson, Smith & Yoedicke Stanford Graduate Fellowship. M.L.B. acknowledges Research Foundation–Flanders (FWO; grant V417018N) for a travel grant to stay at Stanford University. D.P. acknowledges support from Research Foundation–Flanders (FWO; grant 11D4718N). Funding for this work was provided by the National Science Foundation (grant CHE-1660611 to E.I.S.), the Stanford Woods Institute (to E.I.S) Research Foundation–Flanders (grants G0A2216N to B.F.S and R.A.S.). We thank Julien Devos and professor Michiel Dusselier for their synthesis of the chabazite materials used in this work.

Author contributions: B.E.R.S., M.L.B., R.A.S., B.F.S., and E.I.S. designed the research. B.E.R.S, M.L.B., H.M.R., and D.P. performed experiments. B.E.R.S. performed the DFT calculations. B.E.R.S., M.L.B., H.M.R., B.F.S., R.A.S., and E.I.S. analyzed the data. B.E.R.S., M.L.B., H.M.R., and E.I.S. wrote the manuscript.

Competing interests: The authors declare no competing interests.

Data and materials availability: All spectroscopic data presented in the main text are made freely available through Zenodo.[39]

SUPPLEMENTARY MATERIALS

Materials and Methods

Sample Preparation. H-*BEA was prepared from commercial CP814E NH_4-*BEA zeolite by calcination in static air at 550°C, as in refs. (6) and (7). H-CHA zeolite used for the preparation of the Fe-CHA samples was prepared following the CBV720 recipe with N,N,N-trimethyl-1-admantylammonium cations ($TMAda^+$) template from ref. (34). A molar batch composition of 1 Si : 0.067 Al : 0.22 $TMAda^+$: 0.13 Na^+ : 0.35 OH^- : 24.5 H_2O was targeted using zeolite Y (Zeolyst international CBV720) as the Si and Al source. 28.69 g of aqueous N,N,N-trimethyladamantylammonium hydroxide (TMAdaOH) solution (25 wt %, Sachem), 5.29 g of NaOH solution (15 wt%, from >98 wt% NaOH pellets, Sigma Aldrich) and 40.58 g of deionized water (18.2 MΩ cm) was mixed in a 125 ml Teflon lined stainless steel autoclave (Parr Instruments) and homogenized. 11.25 g of the zeolite Y precursor was then added and the mixture was stirred for 2 hours at ambient conditions. The autoclave was then sealed off and oven-heated at 160 °C for 4 days under static conditions.

Fe-CHA and Fe-*BEA materials were prepared by a strategy analogous to the samples in refs (6), (7), and (35): Fe was introduced into dried H-CHA and H-*BEA by diffusion impregnation in a solution of $^{57}Fe(acac)_3$ in toluene (25 mL/g zeolite). The concentration of $^{57}Fe(acac)_3$ in toluene is approximately 0.01 M. All samples were calcined in air with a heating ramp of 2 °C/min to 550 °C for 30 hours to remove organic

material. Each sample is then introduced into a quartz U-tube/flow cell and heated at 10°C/min in a dried 30 ml/min flow of helium (99.999% purity, O_2 filtered with an Agilent 17970 system, H_2O filtered with an Agilent 17971 system) to 900°C where it is kept for one hour. The Fe-*BEA and Fe-CHA materials studied here were compositionally similar with Si/Al ~ 10 and ~0.30 wt.% Fe. Sample specific Si/Al and iron loadings are given in the main manuscript.

N_2O Activation and CH_4/H_2 Reactions. ~0.5g of Fe zeolite is introduced into a quartz U-tube/flow cell. After heating to 900°C in helium (*vide supra*), a 35% N_2O (99%, IJsfabriek Strombeek) in He flow is passed over the sample (20 min at 160°C for Fe-*BEA, 25 min at 180°C for Fe-CHA to achieve maximal α-Fe(IV)=O and minimal spectator). The reactor is flushed in helium at room temperature and a 20 mL/min flow of CH_4 (99.995%, Air Liquide) or H_2 (99.99%, Air Liquide) is passed through the flow cell at room temperature for 5 minutes, followed by another flush in helium. For the isotope labelled experiments CH_4 and H_2 were replaced by 99% labeled $^{13}CH_4$ (99%, 99 atom% ^{13}C, Sigma Aldrich) and D_2 (99%, 99.9 atom% D, Sigma Aldrich) respectively.

Catalyst Cycling Tests. A known amount of Fe-*BEA or Fe-CHA was put into a quartz reactor. The sample was pretreated in a dried helium flow at 900°C, then a 35% N_2O/He atmosphere (large molar excess of N_2O over iron) was inserted into the reactor at room temperature. The reactor was heated in the oven for 30 minutes at 180 °C for Fe-CHA and 160 °C for Fe-*BEA to ensure full oxidation. Then the N_2O/He was removed at room

temperature by a vacuum, and replaced by a 1.5 bar $^{13}CH_4$ atmosphere (99% ^{13}C labeled). After 15 minutes all $^{13}CH_4$ was removed by a vacuum. For the single cycle experiments, methanol was extracted at this point in a 35 ml/min He stream that passed through a bubbler with water at room temperature. The outflow was monitored by in line mass spectrometry using an Omnistar Pfeiffer Vacuum GSD 30102 quadrupole mass spectrometer. For a second cycle experiment, the $^{13}CH_4$ atmosphere was removed by vacuum and replaced by 35%N_2O/He. The reactor was heated in the oven for 15 minutes at 180 °C for Fe-CHA and 160 °C for Fe-*BEA. Then the N_2O/He was removed at room temperature by a vacuum, and replaced by a $^{12}CH_4$ atmosphere. After 15 minutes methanol extraction was started. Different N_2O activation temperatures and durations were tested to optimize for α-Fe(II) conversion and minimize overoxidation of first cycle oxidation products. Quantification of ^{13}C and ^{12}C methanol products was calibrated by a known amount of methanol adsorbed onto Fe-CHA and Fe-*BEA and then extracted using the same procedure as for the reactive cycles. Exemplary mass spectrometry data are shown in Fig. S6. Mass spectrometry during CH_4 reaction did not detect the gas phase release of methanol or other oxidation products. Products other than methanol were also not detected in quantifiable amounts during the steaming procedure. Nevertheless, the methanol yields (both ^{13}C and ^{12}C) are ~30% below what is expected based on Mössbauer spectroscopy. We explain this by the sampling for Mössbauer from the part of the zeolite bed that is least exposed to contaminants. The Mössbauer data therefore does not quantitatively but only relatively represent the whole zeolite bed used for the reactivity tests.

Steam assisted extractions were similar for H and Na exchanged zeolites and for the CHA and BEA topologies (Fig. S7). Although the time required for methanol recovery differs markedly, the final outcome is similar for the purpose of this work.

DR-UV-vis Spectroscopy. Diffuse reflectance spectroscopy in the UV–vis–NIR energy range was performed with a Varian Cary 5000 UV-vis-NIR spectrophotometer at room temperature against a Halon white reflectance standard in the 4000-40000 cm^{-1} energy range. All treatments before UV-vis-NIR spectroscopic measurements were performed in a quartz U-tube/flow cell, equipped with a window for *in situ* measurements.

Mössbauer Spectroscopy. ^{57}Fe Mössbauer spectra were recorded with a See Co. W302 resonant gamma ray spectrometer in horizontal geometry at room temperature with zero external field using a 1.85 GBq source (Be window, Rh matrix). Data were collected from samples enriched with 100% ^{57}Fe. Isomer shifts are given relative to α-iron foil at room temperature. Spectra were collected with 1024 points and summed up to 512 points before analyzing. Spectra were fit to Lorentzian doublets and hyperfine-split multiplets using the Vinda software package for Microsoft Excel. Hyperfine features were fit using a spin Hamiltonian model (SPINHAM), using a vanishingly small external field. A slowly relaxing S=5/2 model was required to fit the data. First, the α-Fe(III)-OH component of H_2-reacted BEA was considered. Its isomer shift, quadrupole splitting, and hyperfine coupling tensor (constrained to be isotropic) were determined from the position of peripheral spectral lines, where there are no contributions from overlapping Lorentzian

components (i.e. above 4 mm/s and below -2 mm/s). The *g* tensor was constrained to be isotropic, with *g=2.*0023. The axial and rhombic zero-field splitting parameters *D* and *E* (respectively) were then floated to properly model the intensity distribution among these peripheral spectral lines, accounting for the 6K sample temperature. For the CH_4 reacted sample, the features of α-Fe(III)-OH were subtracted from the experimental data to facilitate fitting of the remaining α-Fe(III)-OCH_3 component.

Resonance Raman Spectroscopy. Resonance Raman (rR) spectra were recorded using a Spex 1877 CP triple monochromator with 1200, 1800, and 2400 grooves/mm holographic spectrograph gratings and an Andor Newton CCD cooled to –80 °C. Excitation was provided by either a Coherent I90C–K Kr+ ion laser (λ_{ex} = 407) or an Innova Sabre 25/7 Ar+ CW ion laser (λex = 458, 502 nm). The spectral resolution was ~2 cm^{-1}. Spectra were recorded at room temperature, using 20 mW of laser power at the sample. Baseline spectra were collected from samples of α-Fe(IV)=O in BEA and CHA lattice.

Spectroscopic Studies of Fe-CHA. Mössbauer data from the H_2 and CH_4 reactions in CHA are presented in Fig. S1. For the H_2 reaction, α-Fe(IV)=O (initially 84%) is converted into a new majority Fe(III) component (51% of Fe) with hyperfine structure. Based on its resemblance to α-Fe(III)-OH in BEA, as well as rR data (see Fig. S5), we assign this as the CHA α-Fe(III)-OH site (solid black trace, 61% of α-Fe(IV)=O). Some α-Fe(II) is also regenerated (21% of α-Fe(IV)=O). The reaction of α-Fe(IV)=O with H_2 therefore gives a

similar distribution of Fe species in CHA and BEA. For the CH_4 reaction, however, only ~60% of the α-Fe(IV)=O is converted into α-Fe(III)-OH/α-Fe(III)-OCH_3. Unlike BEA, a significant portion (~40% of α-Fe(II)) is regenerated.

DR-UV-vis data from H_2- and CH_4-reacted CHA are presented in Fig. S5. As with BEA, reacting CHA with H_2 at 300 K (Fig. S5d) results in decay of the α-Fe(IV)=O band (17,500 cm^{-1}, gray trace), and leaves a rising slope with somewhat diminished Abs intensity from 20,000-30,000 cm^{-1}. For the CH_4 reaction (Fig. S5e), there is additional Abs intensity at ~22,000 cm^{-1}. Finally, a low energy band appears at 15,000 cm^{-1} that is not present in the BEA sample. However, heating the sample to 450 K results in loss of this absorption feature, but with minimal change to its Mössbauer spectrum, suggesting this is due to a small quantity (<5%) of a strongly absorbing species. Tuning a laser (ν_{ex}=21,800 cm^{-1}) into the Abs shoulder of the H_2-reacted sample resonance enhances a single vibration at 730 cm^{-1} (Fig. S5f, blue trace). We assign this to the α-Fe(III)-OH species. No α-Fe(III)-OH/α-Fe(III)-OCH_3 features are resolved in the CH_4 reacted CHA sample (Fig. S5f, red trace). This is a key difference between CHA and BEA – consistent with Mössbauer data, which show a greatly diminished contribution from Fe(III) species in CH_4-reacted CHA.

Computational Details. Spin-unrestricted DFT calculations were performed using Gaussian 09.(36) Cluster models were generated from crystallographic coordinates of BEA polymorph A (28) and CHA,(37) and dangling Si-O groups were replaced with capping hydrides at 1.42 Å (see supplementary tables 1-17 for coordinates). The B3LYP

functional was used for all calculations. For geometry optimizations and frequency calculations, the 6-311G* basis set was used for Fe, all atoms directly coordinated to iron, and all atoms of the CH_4 substrate. The 6-31G* basis set was used on all other atoms. For geometry optimizations, the six T-sites of the 6-membered ring hosting the iron center, and all atoms of the substrate were allowed to relax. All other atoms were constrained to their crystallographic positions. The stability of all optimized geometries were confirmed by frequency calculations. Guess transition state structures were located through linear transits of the Fe-$OH\cdots CH_3$ distance, and then geometry optimized. Transition state structures were validated through frequency calculations, which showed a single imaginary frequency corresponding to motion along the reaction coordinate. Single point calculations were performed on optimized structures using the 6-311G+* basis set on all atoms, and including the D3 dispersion correction of Grimme in the DFT functional.(38) All single point energies were corrected for thermal contributions to enthalpy and Gibbs free energy at 300K. Mössbauer isomer shifts and quadrupole splittings were calculated according to previously reported methods.(6)

Supplementary Figures

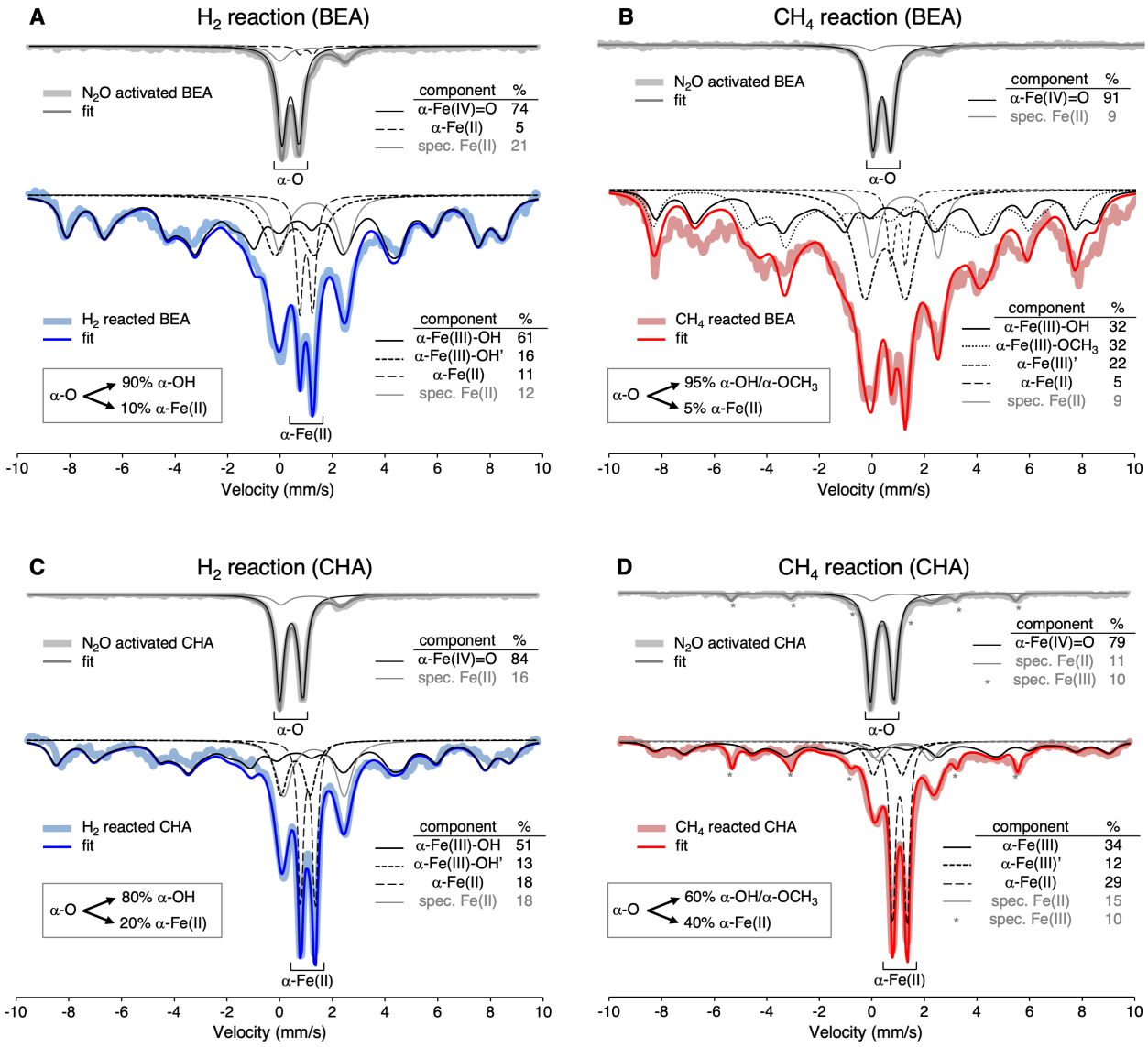

Figure S1. ^{57}Fe Mössbauer spectra of H_2- and CH_4-reacted Fe-CHA and Fe-BEA. Data were collected at 6K. Components of each fit are indicated in the figure legends. Data from the corresponding α-Fe(IV)=O samples are presented above the spectrum of each reacted material (**A** – H_2-reacted BEA, **B** – CH_4-reacted BEA, **C** – H_2-reacted CHA, **D** – CH_4-reacted CHA).

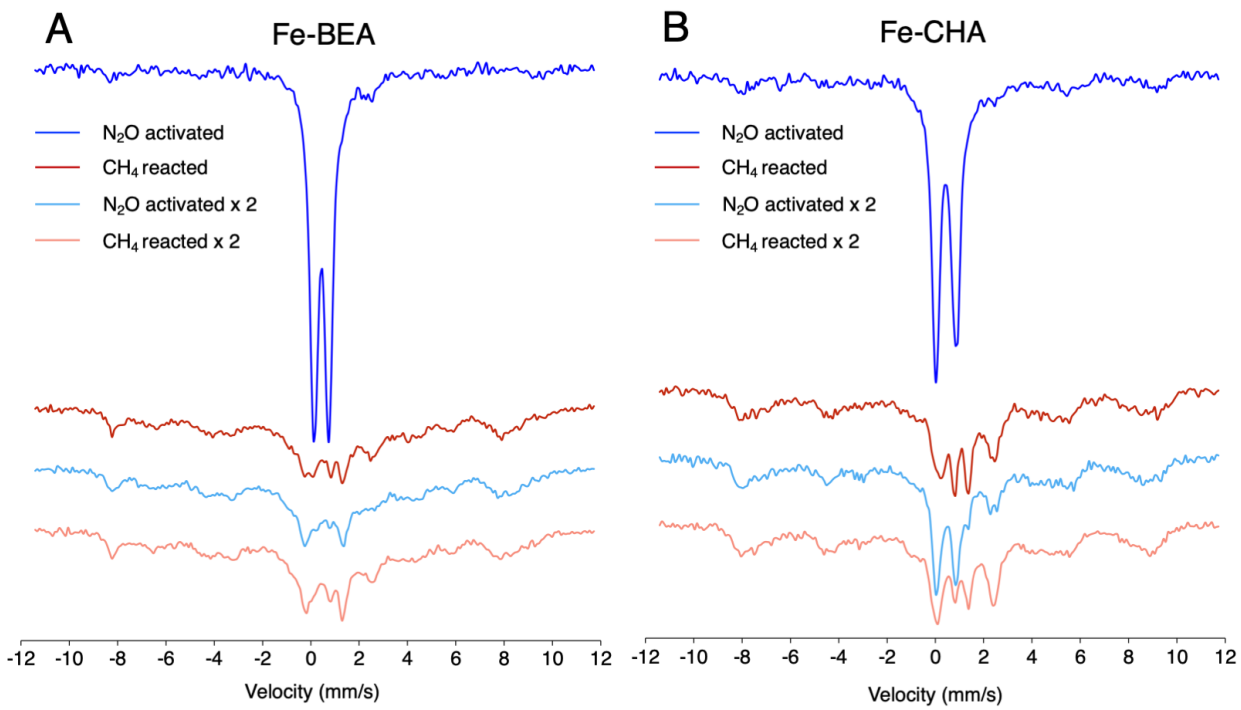

	component	BEA (%)	CHA (%)
N_2O activated	α-Fe(IV)=O	90	74
	α-Fe(III)	0	0
	α-Fe(II)	0	0
CH_4 reacted	α-Fe(IV)=O	0	0
	α-Fe(III)	85	46
	α-Fe(II)	5	28
N_2O activated x 2	α-Fe(IV)=O	0	22
	α-Fe(III)	90	52
	α-Fe(II)	0	0
CH_4 reacted x 2	α-Fe(IV)=O	0	0
	α-Fe(III)	90	54
	α-Fe(II)	0	20

Figure S2. Normalized 6K Mössbauer spectra from **(A)** Fe-*BEA and **(B)** Fe-CHA collected over the course of catalyst cycling. Note regeneration of α-Fe(IV)=O upon reoxidation in Fe-CHA, but not Fe-*BEA (see pale blue traces). **(C)** Active site speciation over the course of catalyst cycling, as quantified from Mössbauer data in panels A and B. These values are associated with errors of ±5%.

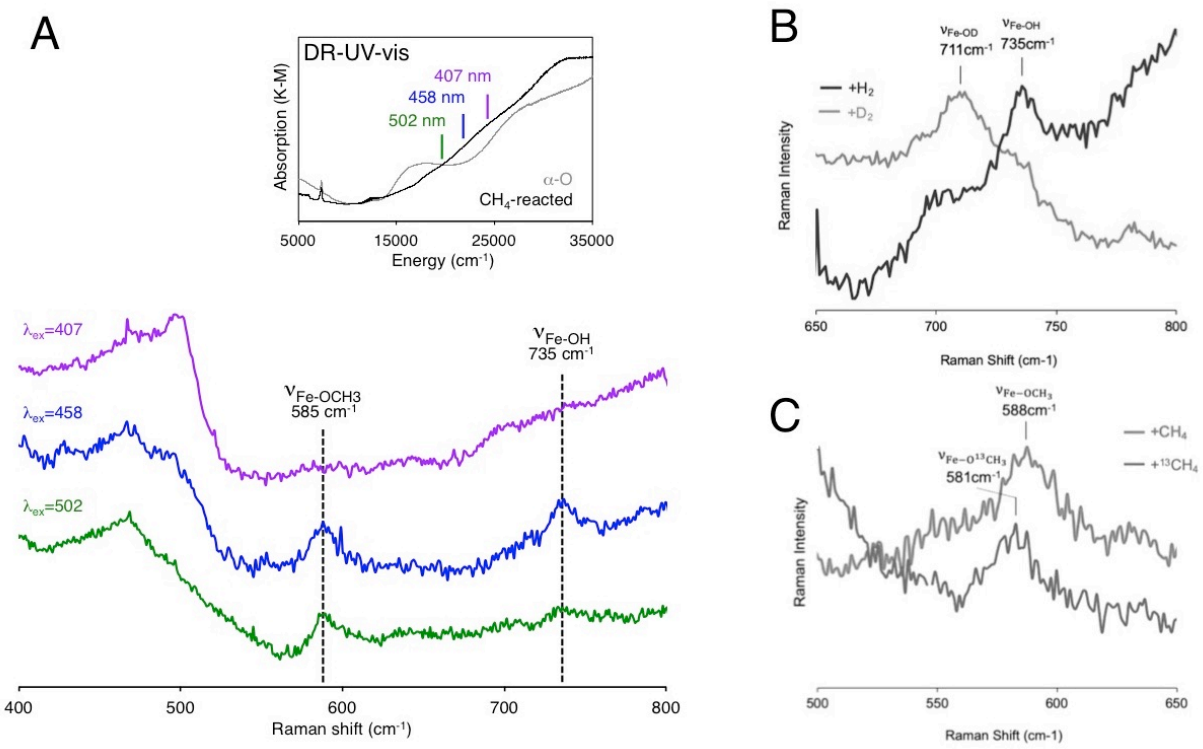

Figure S3. (A) Resonance Raman profile of the characteristic vibrations of α-OH and α-OCH_3 in CH_4-reacted Fe-BEA. The intensities of both features are maximized using an excitation wavelength of 458 nm, indicating these Raman features are in resonance with electronic absorption bands within the 407-502 nm interval. To the right, isotopically perturbed resonance Raman data (λ_{ex}=458 nm) are presented, focusing on the H/D sensitivity of the Fe-OH stretch of α-OH in H_2/D_2-reacted Fe-BEA (**A**), and the $^{12}C/^{13}C$ sensitivity of the Fe-OCH_3 stretch of α-OCH_3 in $^{12}CH_4/^{13}CH_4$-reacted Fe-BEA (**B**). The hydrogen and methane reactions were all performed at 300K.

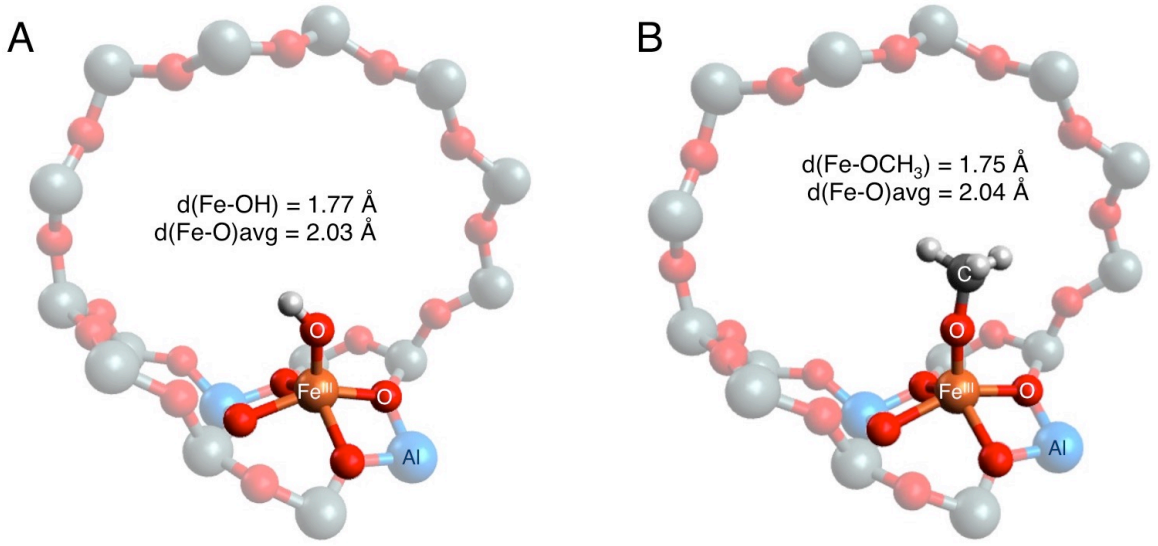

	Mössbauer parameters		$\nu_{Fe\text{-}OH}$ (ΔH/D)
α-OH	**IS (mm/s)**	**QS (mm/s)**	**(cm^{-1})**
EXP	0.5±0.1	-1.6±0.1	735 (24)
DFT	0.41	-1.41	764 (32)

	Mössbauer parameters		$\nu_{Fe\text{-}OH}$ ($\Delta^{12}C/^{13}C$)
α-OCH$_3$	**IS (mm/s)**	**QS (mm/s)**	**(cm^{-1})**
EXP	0.5±0.1	-1.6±0.1	585 (7)
DFT	0.47	-1.34	577 (6)

Figure S4. S=5/2 DFT models of α-OH **(A)** and α-OCH$_3$ sites **(B)** in Fe-BEA, including a comparison of their experimental and calculated spectroscopic features in Mössbauer (IS = isomer shift, QS = quadrupole splitting) and resonance Raman spectroscopy. Atoms have been omitted for clarity.

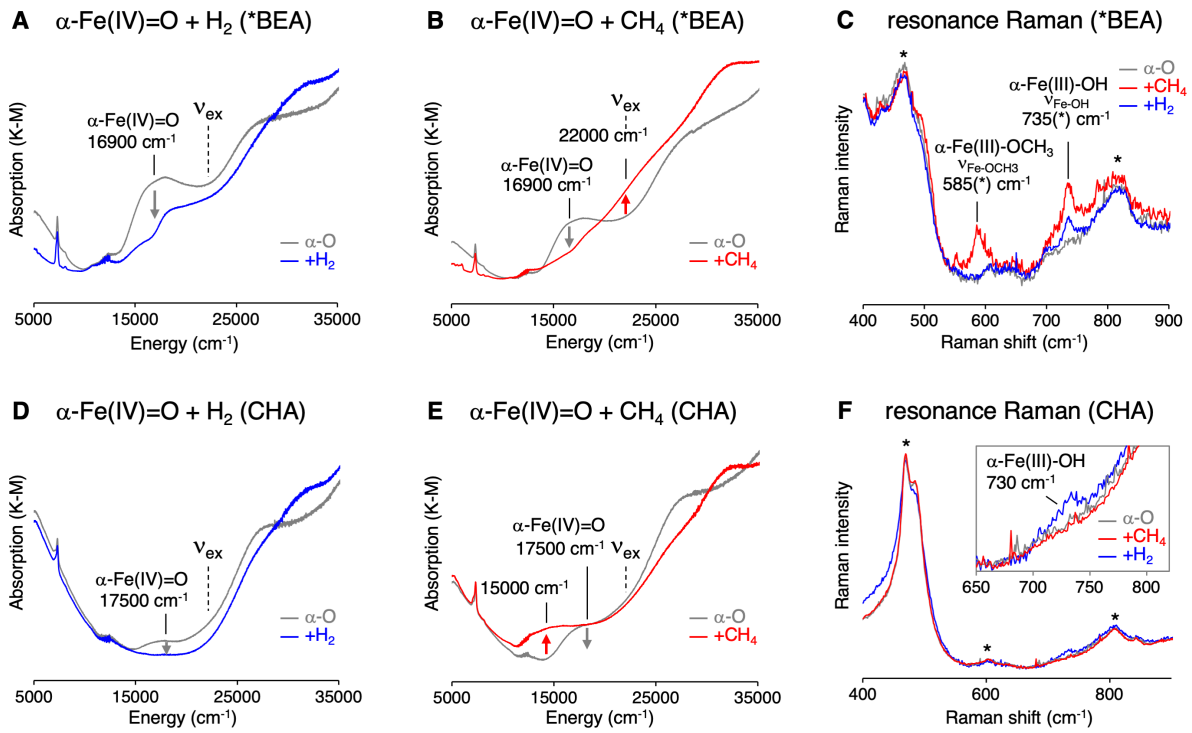

Figure S5. Comparison of DR-UV-vis and rR data (λ_{ex}=458 nm) from H_2/CH_4 reacted BEA (top) and CHA (bottom). All reactions were performed at 300 K. While rR features of the cage escape products α-Fe(III)-OH and α-Fe(III)-OCH_3 are observed in CH_4-reacted BEA (panel C), these species are not detected in CH_4-reacted CHA. Cage escape products are only observed for the smaller substrate H_2 (panel F). Starred features are non-resonant Raman vibrations of the zeolite lattice.

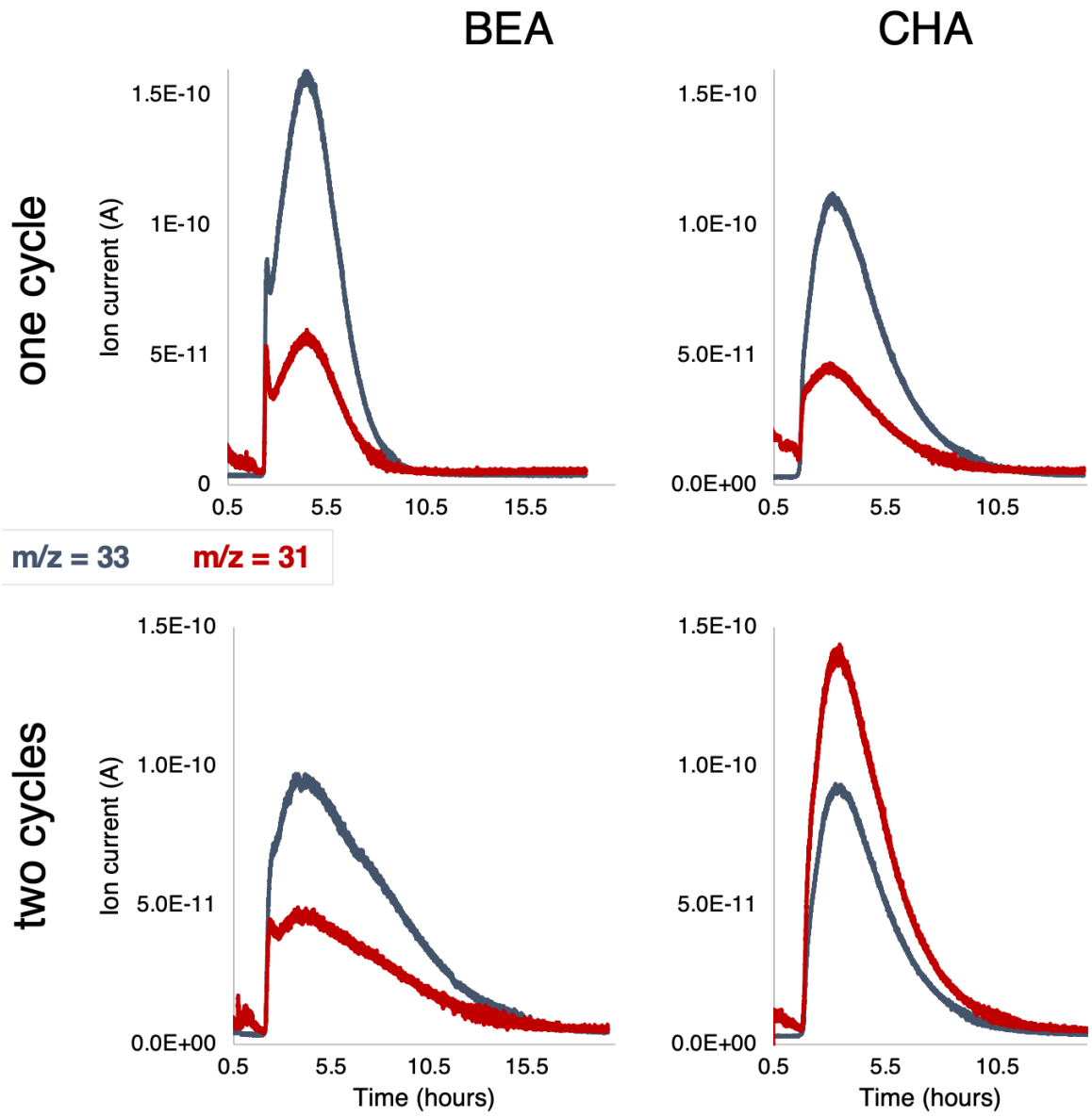

Figure S6. Selected mass spectrometry data used to quantify the steam desorbed $^{13}CH_3OH$ and $^{12}CH_3OH$. m/z=33 was used to quantify $^{13}CH_3OH$. The portion of the m/z=31 signal attributed to $^{13}CH_3OH$ was subtracted from the total signal to quantify $^{12}CH_3OH$.

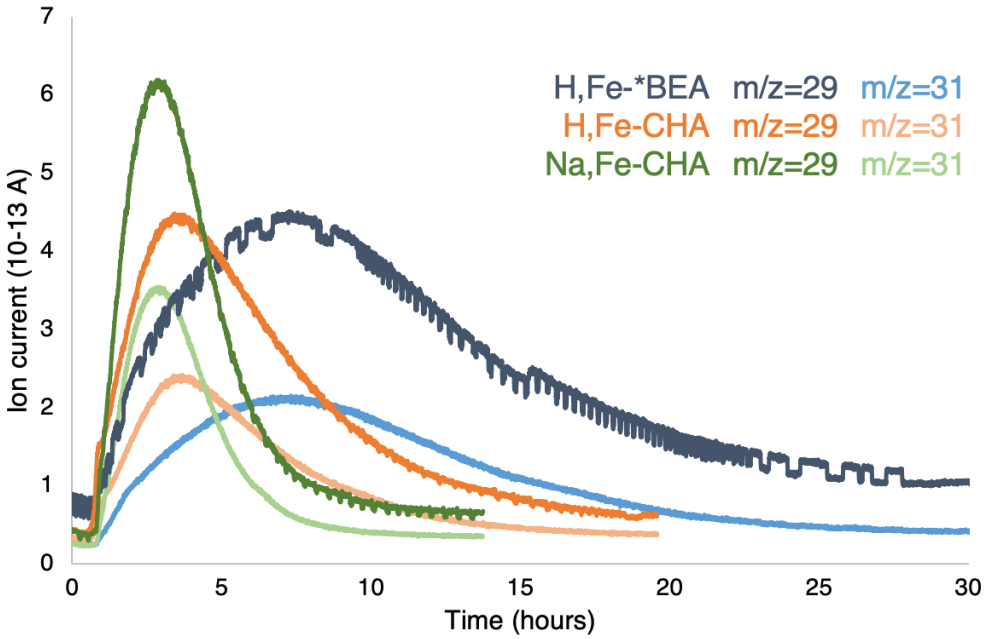

Figure S7. Methanol desorption by a flow of 30 mL/min He saturated with H_2O at room temperature compared for the *BEA vs. CHA topologies and for Na^+ vs H^+ exchanged CHA. Methanol was produced by a reaction of α-O with methane at room temperature.

Supplementary Tables

Table S1 – Coordinates for DFT Model of α-OH···CH_3 Complex (BEA)

element	constrained during optimization?	X	Y	Z
Fe	N	-0.88317713	0.2078925	-0.30780668
O	N	-1.0400598	-0.44184015	1.60450329
O	N	-2.37687441	0.25268539	-1.68318867
O	N	-1.93334343	1.88022371	0.21946534
O	N	-0.84106095	-1.84277563	-0.51339426
O	N	0.75101568	0.71266097	-0.72332064
H	N	1.65230655	0.48644183	-0.43617148
C	N	3.21305879	-0.24578148	0.88023069
H	N	3.13304826	0.65959271	1.46811711
H	N	2.65000536	-1.12165503	1.17712814
H	N	4.03337029	-0.34787691	0.18140014
O	Y	4.87661135	-4.44257331	0.30163545
O	Y	1.27825899	5.77135874	0.64899151
O	Y	6.93006414	-2.79880345	0.15694788
O	Y	6.04196136	4.42530407	0.03027365
O	Y	3.71060695	5.56193854	-0.34005062
O	Y	7.15463405	2.24695049	-0.92669782
O	Y	7.53770541	-0.32180801	-0.50751246
Si	Y	3.32319985	-4.86647248	0.25003353
Si	Y	-0.31975761	5.56885478	0.68192352
Si	Y	5.98373678	-3.79995768	-0.67419749
Si	Y	7.30423865	3.43501077	0.1455109
Si	Y	2.38113727	6.46630161	-0.29602195
Si	Y	7.58505566	0.85172085	-1.60825877
Si	Y	8.11782004	-1.71583324	0.05034822
Si	Y	5.203328	5.41191462	-0.93008396
O	Y	2.57809006	-4.33650714	1.57477511
Si	Y	1.20514996	-4.24318502	2.41140011
H	Y	0.72498441	0.22216818	6.48083059
O	Y	2.63218595	-4.22169495	-1.05123203
H	Y	-0.86362965	5.85729448	-0.59768194
H	Y	7.37260057	2.89143817	1.455571
H	Y	2.99572467	-3.2083064	-3.28320658
H	Y	8.68835307	-1.51596069	1.3352399
H	Y	8.48622223	4.17916665	-0.11053247
H	Y	5.3278827	-3.0748261	-1.70396832
H	Y	1.8632252	6.57139177	-1.61401213

H	Y	6.76597082	-4.83091757	-1.25868583
H	Y	2.7000874	7.75475836	0.20850288
H	Y	9.11683636	-2.20172141	-0.83411566
H	Y	8.90445043	0.97342957	-2.11893871
H	Y	5.15098332	4.8672679	-2.24043
H	Y	6.68520139	0.54664373	-2.66351801
H	Y	5.82687181	6.68694693	-0.97356146
Si	Y	2.02476692	-3.89163911	-2.50423579
O	N	-0.0069791	0.02802504	4.05761858
O	N	-2.84524028	-0.01262259	-4.33628098
H	Y	0.81254472	-1.82960421	5.40400638
H	Y	3.22908059	-6.28209649	0.18842809
H	Y	-4.21283594	4.21609455	-4.11866462
H	Y	1.50081345	-4.13868655	3.79622425
H	Y	-2.61179643	5.31420437	-2.85074504
H	Y	-1.23152514	-0.95737013	6.07445221
H	Y	-5.25708837	-0.3330108	-5.11446855
H	Y	-3.94173059	-1.20644052	5.29758307
H	Y	-6.61689752	-1.55802481	-2.95555335
H	Y	1.66300639	-5.09938037	-3.15758428
H	Y	-0.88434447	6.44110335	1.64980538
O	N	0.78236699	-2.83971473	-2.37288099
O	N	-0.550889	3.99749498	1.05214991
O	N	-0.93329768	1.99026324	2.65089395
O	N	-1.50007281	-1.82494797	-3.06699486
O	N	-2.63925551	0.20452577	3.67742707
O	N	-4.12166885	-1.59107063	-2.61180931
H	Y	-5.1244251	0.2113667	3.88579629
H	Y	-5.73872247	-3.08613362	-1.44034967
O	Y	-4.15970964	-1.85095029	2.91533171
H	Y	-4.80957296	5.15973295	2.809539
O	Y	-5.82528084	-0.70576163	-0.76809888
H	Y	-2.08634563	-6.59763456	-1.71124899
O	N	-4.70897598	1.68675949	-0.4926341
H	Y	-1.75220556	-5.4596028	0.27397778
O	N	-2.24472889	-3.16715043	1.60942187
H	Y	-5.02787416	4.0636545	0.78497986
O	N	-3.00128128	3.00435962	-2.32174871
H	Y	0.43034821	-5.41048192	2.17983227
O	N	0.53591137	-2.83783967	1.94158606
H	Y	-4.71832796	4.91717127	-1.96710834
H	Y	-6.15080497	0.70660986	1.23869362
H	Y	-3.6842613	-5.0945297	-0.96606054

H	Y	-4.62910758	-3.55124479	1.17848673
H	Y	-5.30802453	2.89734291	2.77622182
H	Y	-7.16041854	1.3818953	-0.73616746
O	N	-1.45110768	-4.16661595	-1.81069443
H	Y	-3.77103589	-4.28139872	3.20479645
O	N	-2.96527547	3.60161245	2.07384681
Si	Y	0.05712837	-0.63874217	5.57023429
Si	Y	-4.01817743	0.26379672	-5.46850182
Si	N	-1.17249889	0.42884422	3.02084121
Si	N	-2.74459067	-0.78988245	-2.93008988
Si	Y	-4.01005516	-0.6628577	3.98750595
Si	Y	-5.62852639	-1.76838418	-1.95787707
Al	N	-3.13641855	1.81341683	-1.13164839
Al	N	-0.88302309	-2.21720719	1.25138142
Si	Y	-6.00443507	0.78041402	-0.17182709
Si	Y	-2.29210997	-5.36549847	-1.03598896
Si	Y	-3.72923507	-3.24613987	2.23378664
Si	Y	-4.58582977	3.93410279	2.12818444
Si	N	-1.63279803	2.89898729	1.49627949
Si	N	-0.75964507	-2.71296991	-1.92531086
Si	Y	-3.69769648	4.40016792	-2.80825149
H	Y	-4.16301828	1.67580886	-5.50964355
H	Y	-3.61030004	-0.20749562	-6.74441532

Table S2 – Coordinates for DFT Model of α-Fe(II) (BEA)

element	constrained during optimization?	X	Y	Z
Fe	N	-1.12883888	0.10320115	-0.21656273
O	N	-0.95669034	-0.46232606	1.67806171
O	N	-2.38006755	0.28004486	-1.74770877
O	N	-1.87230785	1.92004893	0.18314947
O	N	-0.72559543	-1.84267712	-0.49485712
O	Y	4.94558774	-4.43295001	0.3203729
O	Y	1.34801784	5.78217523	0.63992601
O	Y	6.99958707	-2.78975642	0.17683658
O	Y	6.11283216	4.43421721	0.03404538
O	Y	3.78244321	5.57045776	-0.34349751
O	Y	7.22722346	2.25382251	-0.91625629
O	Y	7.60901638	-0.31416147	-0.49119815
Si	Y	3.39223206	-4.85672332	0.26628911

Si	Y	-0.25008882	5.57997464	0.66984097
Si	Y	6.05488926	-3.79240787	-0.65435803
Si	Y	7.37471357	3.44397058	0.15392925
Si	Y	2.45301683	6.47509881	-0.30409032
Si	Y	7.65889313	0.85719167	-1.59414893
Si	Y	8.18772954	-1.70716996	0.07064424
Si	Y	5.27640016	5.41905698	-0.9300427
O	Y	2.64438202	-4.32405323	1.58840047
Si	Y	1.26966375	-4.22887428	2.42188553
H	Y	0.78145736	0.24455456	6.48148439
O	Y	2.704092	-4.21439524	-1.03772303
H	Y	-0.7911904	5.8659687	-0.61148552
H	Y	7.44019418	2.90296724	1.46520016
H	Y	3.07254949	-3.20546414	-3.27090739
H	Y	8.75554567	-1.50485016	1.35635652
H	Y	8.55735233	4.18745002	-0.10105195
H	Y	5.40134515	-3.06921069	-1.68695405
H	Y	1.93793779	6.57766828	-1.62338951
H	Y	6.83821786	-4.82462959	-1.23514268
H	Y	2.77107989	7.76449924	0.19857752
H	Y	9.18856242	-2.19494208	-0.81072449
H	Y	8.9793949	0.97770386	-2.10224611
H	Y	5.22677505	4.87183918	-2.23942399
H	Y	6.76125093	0.55016805	-2.6507268
H	Y	5.90022515	6.69391106	-0.97469686
Si	Y	2.09982881	-3.88711335	-2.49267638
O	N	0.06284683	0.10200961	4.0902585
O	N	-2.74467337	-0.04704576	-4.38211772
H	Y	0.87101099	-1.80934599	5.40888958
H	Y	3.29801954	-6.27244536	0.20725802
H	Y	-4.13311217	4.21832532	-4.13638188
H	Y	1.56236278	-4.12169756	3.80713269
H	Y	-2.53461622	5.31869375	-2.86721211
H	Y	-1.1743574	-0.93549513	6.07324611
H	Y	-5.17590393	-0.33258811	-5.12546182
H	Y	-3.8829308	-1.18570719	5.29107787
H	Y	-6.54051057	-1.55314484	-2.96704774
H	Y	1.73928256	-5.09609267	-3.14441136
H	Y	-0.81661821	6.45420081	1.63480057
O	N	0.8586752	-2.82983618	-2.37915712
O	N	-0.4764637	4.00451433	1.03000645
O	N	-0.88270978	2.00231555	2.62543751
O	N	-1.42427486	-1.81339575	-3.04023414

O	N	-2.58215821	0.23701016	3.69301448
O	N	-4.05908255	-1.6092377	-2.650114
H	Y	-5.062398	0.22949071	3.87398002
H	Y	-5.66580375	-3.07839904	-1.44696866
O	Y	-4.09591657	-1.83487079	2.90963848
H	Y	-4.74451271	5.17568389	2.7886595
O	Y	-5.75344016	-0.69669442	-0.77959309
H	Y	-2.01337515	-6.59095677	-1.70314456
O	N	-4.64751236	1.71438462	-0.50138873
H	Y	-1.68330782	-5.44906365	0.2805449
O	N	-2.18808524	-3.15412089	1.58526527
H	Y	-4.95864676	4.07565573	0.76579898
O	N	-2.91396278	3.01176417	-2.36281586
H	Y	0.49517078	-5.39650471	2.1909498
O	N	0.60414085	-2.82216998	1.98361439
H	Y	-4.64309021	4.92370948	-1.98729486
H	Y	-6.0830435	0.71966884	1.22371881
H	Y	-3.61265717	-5.08615517	-0.96433631
H	Y	-4.56185308	-3.5385155	1.17514492
H	Y	-5.24322414	2.91330441	2.75872925
H	Y	-7.08833766	1.39120941	-0.75461774
O	N	-1.37448548	-4.16001761	-1.80276527
H	Y	-3.70822355	-4.26480121	3.20471866
O	N	-2.89643547	3.63232163	2.05714146
Si	Y	0.1154217	-0.61804675	5.57115903
Si	Y	-3.936152	0.26334971	-5.47803034
Si	N	-1.10792523	0.45214418	3.04892912
Si	N	-2.6884559	-0.79859526	-2.962902
Si	Y	-3.9483813	-0.64468503	3.97979586
Si	Y	-5.55430415	-1.76170588	-1.96685747
Al	N	-3.08729187	1.84254904	-1.16560541
Al	N	-0.80153797	-2.21992559	1.28072638
Si	Y	-5.93366132	0.79069511	-0.18661926
Si	Y	-2.22040236	-5.35747053	-1.03075807
Si	Y	-3.66418475	-3.23146486	2.23176469
Si	Y	-4.51950263	3.94869207	2.1102012
Si	N	-1.57262015	2.91939965	1.47686939
Si	N	-0.67700176	-2.71078598	-1.9112984
Si	Y	-3.62074899	4.40491193	-2.82525113
H	Y	-4.08069853	1.67529606	-5.52224516
H	Y	-3.52562135	-0.21050944	-6.75213146

Table S3 – Coordinates for DFT Model of α-O (BEA)

element	constrained during optimization?	X	Y	Z
Fe	N	-0.91671491	0.17603945	-0.28283458
O	N	-1.00631261	-0.44267911	1.6278311
O	N	-2.3666186	0.23921784	-1.67295926
O	N	-1.86718256	1.85971359	0.21941703
O	N	-0.77442756	-1.80711442	-0.50276371
O	N	0.49253807	0.69473342	-0.80528232
O	Y	4.92431485	-4.45223802	0.32936005
O	Y	1.3408724	5.76730625	0.66532759
O	Y	6.98076239	-2.81167126	0.19090354
O	Y	6.10433749	4.41381069	0.06125501
O	Y	3.77590579	5.55407073	-0.3162491
O	Y	7.21653202	2.23368335	-0.89222701
O	Y	7.59430578	-0.33565401	-0.47178009
Si	Y	3.37040808	-4.87372562	0.27302532
Si	Y	-0.2575663	5.56732953	0.69330328
Si	Y	6.03542263	-3.81137918	-0.64310176
Si	Y	7.36470794	3.42155221	0.18039299
Si	Y	2.44772037	6.46052151	-0.27631782
Si	Y	7.64685949	0.83775567	-1.57241807
Si	Y	8.17053022	-1.73056113	0.08790428
Si	Y	5.27019146	5.40169192	-0.90170181
O	Y	2.62208921	-4.34251704	1.59545854
Si	Y	1.24664945	-4.24693411	2.42782899
H	Y	0.76108173	0.21923792	6.4956374
O	Y	2.6843789	-4.22788486	-1.03037751
H	Y	-0.79706307	5.8565604	-0.58789692
H	Y	7.42820736	2.8779253	1.49067615
H	Y	3.05634753	-3.21516319	-3.26126442
H	Y	8.7374367	-1.53152817	1.37453077
H	Y	8.54863091	4.16385109	-0.07205527
H	Y	5.38385997	-3.08526615	-1.67490273
H	Y	1.9340129	6.56635738	-1.59589864
H	Y	6.81783284	-4.84358316	-1.22515437
H	Y	2.7671369	7.74848819	0.22912946
H	Y	9.17149143	-2.21804387	-0.79347852
H	Y	8.96800176	0.95738286	-2.07905875
H	Y	5.2210107	4.85707511	-2.21218437
H	Y	6.7497663	0.53404203	-2.63041758
H	Y	5.89585615	6.67574742	-0.94331467

Si	Y	2.08196929	-3.89694836	-2.4852466
O	N	0.03480766	0.03465076	4.07609949
O	N	-2.77407588	-0.00927613	-4.33499126
H	Y	0.84872652	-1.83270399	5.41915837
H	Y	3.2742533	-6.28917773	0.21116755
H	Y	-4.13800483	4.22046345	-4.11907612
H	Y	1.53831031	-4.142948	3.81358004
H	Y	-2.5391601	5.31611279	-2.8463067
H	Y	-1.19602386	-0.95726345	6.08332217
H	Y	-5.18632007	-0.32705993	-5.11790854
H	Y	-3.90421286	-1.20213952	5.2981505
H	Y	-6.5546532	-1.54984045	-2.96311442
H	Y	1.72029122	-5.10415226	-3.13966181
H	Y	-0.82373802	6.44047945	1.65950386
O	N	0.83979004	-2.84147363	-2.36105765
O	N	-0.49486008	3.99077958	1.04467572
O	N	-0.88378877	1.99159792	2.65998817
O	N	-1.43836757	-1.81712505	-3.05548652
O	N	-2.59942071	0.21608372	3.68679659
O	N	-4.06796105	-1.60401688	-2.63107386
H	Y	-5.08038665	0.21746078	3.88270789
H	Y	-5.68352521	-3.07927502	-1.44517909
O	Y	-4.1159038	-1.84641691	2.91532497
H	Y	-4.75451019	5.16529369	2.80724728
O	Y	-5.76844832	-0.69873186	-0.77333166
H	Y	-2.03579429	-6.59649371	-1.70475958
O	N	-4.65243556	1.70205473	-0.48579717
H	Y	-1.70596774	-5.45890122	0.28143107
O	N	-2.2109951	-3.15414251	1.58595664
H	Y	-4.96833368	4.06947714	0.78206813
O	N	-2.92765629	3.00833732	-2.31948764
H	Y	0.47082236	-5.41312167	2.19395151
O	N	0.56720348	-2.84587645	1.97128005
H	Y	-4.64900616	4.9224383	-1.9691203
H	Y	-6.09790428	0.71419138	1.23244788
H	Y	-3.63365116	-5.09088331	-0.96451501
H	Y	-4.58266724	-3.54601413	1.17707446
H	Y	-5.25639211	2.9036907	2.77246794
H	Y	-7.10035951	1.39097968	-0.74555779
O	N	-1.40187944	-4.14287071	-1.77417077
H	Y	-3.73190616	-4.27741161	3.20603238
O	N	-2.91309445	3.59164476	2.05443655
Si	Y	0.09461771	-0.6406435	5.58302212

Si	Y	-3.94539248	0.2678036	-5.4681443
Si	N	-1.12707209	0.43391823	3.04182609
Si	N	-2.69429523	-0.79728156	-2.93632018
Si	Y	-3.9677119	-0.65841852	3.98784093
Si	Y	-5.56958208	-1.76176385	-1.96242874
Al	N	-3.08557794	1.8198421	-1.13503489
Al	N	-0.83106996	-2.214622	1.27119934
Si	Y	-5.94707744	0.78775679	-0.17744032
Si	Y	-2.24173864	-5.36394586	-1.03022906
Si	Y	-3.68553141	-3.24229701	2.23497095
Si	Y	-4.53048906	3.93929759	2.12659366
Si	N	-1.57039102	2.89516745	1.49936172
Si	N	-0.69530589	-2.70118635	-1.91430514
Si	Y	-3.6266018	4.40364775	-2.80698067
H	Y	-4.08791191	1.68003488	-5.50979579
H	Y	-3.53435056	-0.20417456	-6.74280757

Table S4 – Coordinates for DFT Model of α-OH (BEA)

element	constrained during optimization?	X	Y	Z
Fe	N	-0.84673097	0.20228632	-0.30335058
O	N	-0.99908053	-0.4371057	1.61115894
O	N	-2.34219503	0.24565126	-1.66945215
O	N	-1.87509261	1.87832175	0.22198741
O	N	-0.78982757	-1.83840538	-0.50020977
O	N	0.75391944	0.69714192	-0.86389625
H	N	1.62063145	0.30266454	-0.98581128
O	Y	4.91208494	-4.45498761	0.33673611
O	Y	1.33281809	5.76581926	0.66872748
O	Y	6.96819533	-2.81525728	0.19921073
O	Y	6.09614477	4.41008206	0.06841789
O	Y	3.7685036	5.55132229	-0.31099179
O	Y	7.20809402	2.22933761	-0.88394042
O	Y	7.58445419	-0.34017503	-0.46307391
Si	Y	3.35784438	-4.87629668	0.27931788
Si	Y	-0.26565355	5.56645528	0.69562488
Si	Y	6.02420609	-3.81524059	-0.63503391
Si	Y	7.35598594	3.41728092	0.18863644
Si	Y	2.44069235	6.45834559	-0.27219654
Si	Y	7.63831714	0.83313276	-1.56362275

Si	Y	8.15972029	-1.73529494	0.09782321
Si	Y	5.2631625	5.39820459	-0.89529839
O	Y	2.6087764	-4.34495309	1.60110359
Si	Y	1.23313356	-4.24823247	2.43266567
H	Y	0.74617268	0.21872493	6.4993101
O	Y	2.67322782	-4.23025274	-1.02468351
H	Y	-0.80411637	5.85578241	-0.58613775
H	Y	7.41825645	2.87379856	1.49903674
H	Y	3.04727877	-3.21797295	-3.25541199
H	Y	8.72551232	-1.53612378	1.38448658
H	Y	8.54042549	4.15902337	-0.06301558
H	Y	5.37373104	-3.08894162	-1.66746883
H	Y	1.92802673	6.56425348	-1.59216619
H	Y	6.80652136	-4.84787423	-1.21609666
H	Y	2.76029263	7.74625617	0.23333591
H	Y	9.16106854	-2.2232972	-0.78303637
H	Y	8.95989318	0.95210804	-2.06928191
H	Y	5.21472924	4.85343799	-2.20574425
H	Y	6.74188902	0.52967562	-2.62226042
H	Y	5.88942157	6.6719782	-0.93660641
Si	Y	2.07203909	-3.89932126	-2.48000431
O	N	0.01969752	0.02586564	4.07447106
O	N	-2.78308135	-0.01081375	-4.33014602
H	Y	0.83372217	-1.83341178	5.42317048
H	Y	3.26129072	-6.29164115	0.21765393
H	Y	-4.14314917	4.22069113	-4.11960376
H	Y	1.52351255	-4.14407387	3.81840425
H	Y	-2.54477643	5.31584783	-2.84577908
H	Y	-1.21114092	-0.95696235	6.08566415
H	Y	-5.19269866	-0.32646414	-5.1186344
H	Y	-3.91886512	-1.20073953	5.29849918
H	Y	-6.56318761	-1.54838179	-2.96473637
H	Y	1.71030646	-5.10635063	-3.13457987
H	Y	-0.83226423	6.44003203	1.66114582
O	N	0.83608434	-2.8348601	-2.3521504
O	N	-0.50217742	3.99515225	1.06128894
O	N	-0.89486463	1.99065543	2.66259589
O	N	-1.4452312	-1.82318199	-3.05391205
O	N	-2.608863	0.2071799	3.67674359
O	N	-4.07134424	-1.59459267	-2.61830977
H	Y	-5.09329881	0.21919578	3.88195363
H	Y	-5.69388047	-3.07799643	-1.44595201
O	Y	-4.12891878	-1.84513323	2.91542377

H	Y	-4.7644209	5.16673254	2.80610548
O	Y	-5.77842685	-0.69735751	-0.77442547
H	Y	-2.04754521	-6.59685054	-1.7023138
O	N	-4.6582699	1.69559204	-0.49115668
H	Y	-1.71869341	-5.45914924	0.28399011
O	N	-2.21766884	-3.15906153	1.60415505
H	Y	-4.97719853	4.07073885	0.78091327
O	N	-2.94114345	3.00552284	-2.31876304
H	Y	0.45661454	-5.41402926	2.1981137
O	N	0.55852339	-2.8461634	1.96834617
H	Y	-4.65544797	4.92313546	-1.97011659
H	Y	-6.10859636	0.71604906	1.23088735
H	Y	-3.64526306	-5.09040451	-0.96347727
H	Y	-4.59520382	-3.54485288	1.17719573
H	Y	-5.26728714	2.90534315	2.77126219
H	Y	-7.10926885	1.39302477	-0.74793448
O	N	-1.40221806	-4.1661173	-1.79712555
H	Y	-3.7463547	-4.27638762	3.20689152
O	N	-2.92171567	3.60099292	2.07049065
Si	Y	0.08007292	-0.64105714	5.58641198
Si	Y	-3.9511515	0.26778246	-5.46799418
Si	N	-1.13649622	0.42960376	3.03134226
Si	N	-2.69403362	-0.79132786	-2.92524023
Si	Y	-3.98112716	-0.65728318	3.98814575
Si	Y	-5.57887893	-1.76051173	-1.9632497
Al	N	-3.0847148	1.81762632	-1.12715349
Al	N	-0.84579878	-2.21498176	1.26809327
Si	Y	-5.95635911	0.78927257	-0.1790747
Si	Y	-2.25341202	-5.36422199	-1.02804471
Si	Y	-3.69876662	-3.24150891	2.23594663
Si	Y	-4.54045264	3.94049848	2.12579388
Si	N	-1.58506172	2.89898877	1.50433197
Si	N	-0.7102836	-2.71373844	-1.9107719
Si	Y	-3.63247027	4.40391989	-2.80719698
H	Y	-4.09310483	1.68008184	-5.50997434
H	Y	-3.5394727	-0.20454351	-6.74231845

Table S5 – Coordinates for DFT Model of α-OCH_3 (BEA)

element	constrained during optimization?	X	Y	Z
Fe	N	-0.8592125	0.19339361	-0.29282275
O	N	-1.02665169	-0.45587964	1.62262601
O	N	-2.35571336	0.2527359	-1.67079623
O	N	-1.91023793	1.87569731	0.24556535
O	N	-0.81393149	-1.85066386	-0.50270537
O	N	0.71212542	0.80126276	-0.75806112
C	N	1.89271544	1.55277248	-0.81872581
H	N	1.74691806	2.52455531	-0.33619774
H	N	2.6979614	1.01736257	-0.30582234
H	N	2.17471855	1.7069376	-1.86479575
O	Y	4.85187037	-4.51956881	0.34093809
O	Y	1.3514797	5.72804685	0.69735929
O	Y	6.92206372	-2.8955436	0.21267284
O	Y	6.10526905	4.3372355	0.10183303
O	Y	3.78727529	5.49765916	-0.27844718
O	Y	7.20206881	2.15082576	-0.85509165
O	Y	7.55764422	-0.42273467	-0.44116205
Si	Y	3.29471279	-4.92811915	0.27929173
Si	Y	-0.24859466	5.54113351	0.72057867
Si	Y	5.97076934	-3.88503545	-0.6267278
Si	Y	7.35714039	3.3343232	0.22137885
Si	Y	2.4664686	6.4148542	-0.23935959
Si	Y	7.62273429	0.75339088	-1.53822606
Si	Y	8.12092499	-1.8239426	0.11595495
Si	Y	5.28180717	5.33471813	-0.86041981
O	Y	2.54728138	-4.39463255	1.60131111
Si	Y	1.17048091	-4.2901793	2.43036983
H	Y	0.71077156	0.16801925	6.50989423
O	Y	2.61745815	-4.27289233	-1.02401209
H	Y	-0.78232624	5.83845894	-0.56121217
H	Y	7.41270855	2.78639604	1.53023099
H	Y	3.00362914	-3.25679959	-3.25095003
H	Y	8.68603628	-1.63330044	1.40464048
H	Y	8.5477755	4.06760739	-0.02579177
H	Y	5.32791694	-3.15060941	-1.65810941
H	Y	1.95714154	6.52873717	-1.55996463
H	Y	6.74622627	-4.92193406	-1.20973864
H	Y	2.7950958	7.69869287	0.27068905
H	Y	9.1201861	-2.3170676	-0.76421824

H	Y	8.94614981	0.86363792	-2.04104525
H	Y	5.2316311	4.7943255	-2.17261107
H	Y	6.72598603	0.46012097	-2.59945992
H	Y	5.91800672	6.60371031	-0.89666762
Si	Y	2.02164933	-3.93282448	-2.47951977
O	N	-0.01244916	-0.00124912	4.08818702
O	N	-2.79913337	0.00034769	-4.32823746
H	Y	0.7844363	-1.881438	5.42765304
H	Y	3.18711889	-6.34255139	0.21304979
H	Y	-4.12721258	4.24009962	-4.10591085
H	Y	1.45930153	-4.19260402	3.81714853
H	Y	-2.52281019	5.31888833	-2.8257601
H	Y	-1.2548174	-0.99117248	6.08900077
H	Y	-5.21013176	-0.29575632	-5.12077167
H	Y	-3.96283659	-1.21153437	5.296014
H	Y	-6.59415231	-1.51350784	-2.97315548
H	Y	1.65181063	-5.13510043	-3.1383686
H	Y	-0.81015792	6.41606766	1.68780397
O	N	0.78674115	-2.87036429	-2.36727561
O	N	-0.48934716	3.96395776	1.07105754
O	N	-0.91171541	1.9704297	2.67848771
O	N	-1.47970367	-1.82545486	-3.05355578
O	N	-2.64000709	0.19495069	3.68379611
O	N	-4.10425229	-1.57395828	-2.62142031
H	Y	-5.12357331	0.22177439	3.88164412
H	Y	-5.73961837	-3.05443606	-1.45741569
O	Y	-4.17348831	-1.84713566	2.91076536
H	Y	-4.75429692	5.16986076	2.82150042
O	Y	-5.80678218	-0.67523329	-0.77884292
H	Y	-2.1201833	-6.60071787	-1.71768811
O	N	-4.67586401	1.71339136	-0.49699566
H	Y	-1.78628746	-5.47162894	0.27266537
O	N	-2.27264688	-3.16338923	1.59324518
H	Y	-4.97171774	4.08172158	0.79257373
O	N	-2.92960176	3.0157564	-2.3025749
H	Y	0.38572539	-5.44926628	2.19102076
O	N	0.50160657	-2.88324973	1.97645762
H	Y	-4.63812438	4.93999698	-1.95525839
H	Y	-6.12995195	0.73452714	1.23018536
H	Y	-3.70758706	-5.08418654	-0.97725187
H	Y	-4.64956709	-3.53779944	1.1663401
H	Y	-5.27459957	2.9125618	2.7787948
H	Y	-7.12159339	1.42524684	-0.74845621

O	N	-1.46330123	-4.16926521	-1.80046721
H	Y	-3.81022177	-4.28203142	3.1953827
O	N	-2.9152999	3.61843152	2.09414905
Si	Y	0.03970907	-0.68370607	5.59304082
Si	Y	-3.96345094	0.28990607	-5.46604215
Si	N	-1.16428047	0.40638095	3.04051947
Si	N	-2.71804872	-0.78319476	-2.92303524
Si	Y	-4.01839862	-0.66351522	3.98715087
Si	Y	-5.61351908	-1.73641399	-1.97052749
Al	N	-3.09519279	1.81956129	-1.11913249
Al	N	-0.8878703	-2.23253576	1.2626404
Si	Y	-5.97478897	0.81095351	-0.17910129
Si	Y	-2.31779361	-5.3685133	-1.04011574
Si	Y	-3.75277689	-3.24453857	2.22748192
Si	Y	-4.53855345	3.94405763	2.13788652
Si	N	-1.59719311	2.88557752	1.52237701
Si	N	-0.75100454	-2.72558608	-1.91204167
Si	Y	-3.61780121	4.41528547	-2.79198805
H	Y	-4.09426421	1.70338198	-5.50390997
H	Y	-3.55291993	-0.18172244	-6.74096699

Table S6 – Coordinates for DFT Model of C-O Recombination TS (BEA)

element	constrained during optimization?	X	Y	Z
Fe	N	-0.88618006	0.20844731	-0.29585694
O	N	-1.05297281	-0.43907767	1.62043272
O	N	-2.37610343	0.24640971	-1.67837952
O	N	-1.94760098	1.8832949	0.2292295
O	N	-0.8105164	-1.83401901	-0.50705038
O	N	0.7422407	0.80886032	-0.67061895
H	N	1.28635252	1.5784887	-0.48836409
C	N	3.10023815	-0.46753597	-0.06997848
H	N	3.70511097	0.33058103	0.3393772
H	N	2.59619764	-1.15529723	0.59363855
H	N	3.08430711	-0.63820456	-1.13550146
O	Y	4.88581737	-4.4356887	0.33753518
O	Y	1.2693725	5.77257892	0.66306481
O	Y	6.93713558	-2.78864727	0.19988652
O	Y	6.03771593	4.43390052	0.06442378
O	Y	3.70600621	5.56644199	-0.31606467

O	Y	7.15778324	2.25668951	-0.88650291
O	Y	7.54337856	-0.31113549	-0.46392635
Si	Y	3.33332698	-4.86217118	0.28001801
Si	Y	-0.32842242	5.56748379	0.68973809
Si	Y	5.99578969	-3.79194864	-0.63432077
Si	Y	7.30114196	3.44576333	0.18543635
Si	Y	2.37489106	6.46865433	-0.27801949
Si	Y	7.5932189	0.86167972	-1.5653236
Si	Y	8.12353394	-1.70380646	0.0972643
Si	Y	5.20132513	5.41844472	-0.90000147
O	Y	2.58205508	-4.33248896	1.60138929
Si	Y	1.20561363	-4.24080822	2.43241844
H	Y	0.70181274	0.22667225	6.49665828
O	Y	2.64647612	-4.2194486	-1.02447904
H	Y	-0.86763969	5.85410793	-0.59224156
H	Y	7.36514055	2.90324274	1.49615322
H	Y	3.0172991	-3.20707544	-3.25571285
H	Y	8.68858311	-1.50207563	1.38428722
H	Y	8.48292186	4.19167374	-0.0664065
H	Y	5.3428826	-3.06863386	-1.66723708
H	Y	1.86209564	6.5719482	-1.59815126
H	Y	6.78204908	-4.82204252	-1.21492242
H	Y	2.68970495	7.75799316	0.22684622
H	Y	9.12688374	-2.18868822	-0.78283635
H	Y	8.91444982	0.98518674	-2.07079884
H	Y	5.15512692	4.87277292	-2.21015288
H	Y	6.6981041	0.55436973	-2.62396009
H	Y	5.82294876	6.69446675	-0.94190231
Si	Y	2.044348	-3.89143313	-2.4801519
O	N	-0.02343086	0.03920489	4.07595948
O	N	-2.82483916	-0.01941877	-4.33373095
H	Y	0.79704803	-1.82572498	5.42167873
H	Y	3.24175998	-6.27798447	0.21904953
H	Y	-4.20001242	4.20488974	-4.12543099
H	Y	1.49553102	-4.13483636	3.81834287
H	Y	-2.60586408	5.30653061	-2.8519049
H	Y	-1.25111937	-0.95636258	6.0832937
H	Y	-5.23280366	-0.34664309	-5.12212104
H	Y	-3.95777358	-1.21044176	5.29574857
H	Y	-6.59925364	-1.57232937	-2.96778438
H	Y	1.68718566	-5.10024112	-3.13406378
H	Y	-0.89831844	6.439491	1.65472275
O	N	0.79761179	-2.8436859	-2.36976179

O	N	-0.54858291	3.98626749	1.04266313
O	N	-0.94753953	1.99513975	2.66018707
O	N	-1.48247513	-1.82758495	-3.05635085
O	N	-2.65538772	0.21028054	3.68437438
O	N	-4.10786966	-1.60221467	-2.61837524
H	Y	-5.13712237	0.20441116	3.87820835
H	Y	-5.72465954	-3.09791174	-1.44797033
O	Y	-4.16514592	-1.85701392	2.91310945
H	Y	-4.82606626	5.15251413	2.79963895
O	Y	-5.81780733	-0.71720236	-0.77779748
H	Y	-2.06547571	-6.60360982	-1.70168176
O	N	-4.71262248	1.68421001	-0.50541892
H	Y	-1.74116117	-5.46360386	0.28404055
O	N	-2.24916821	-3.16045109	1.60090859
H	Y	-5.03444968	4.0546292	0.77501468
O	N	-2.98562377	3.00069945	-2.32022377
H	Y	0.43364559	-5.40953258	2.19858163
O	N	0.52667047	-2.84067493	1.96560567
H	Y	-4.71526782	4.90667936	-1.97642634
H	Y	-6.1536893	0.69606895	1.22665443
H	Y	-3.66882717	-5.10259342	-0.96399565
H	Y	-4.62478903	-3.55932385	1.1756293
H	Y	-5.32066917	2.88928592	2.76596111
H	Y	-7.15648527	1.36827798	-0.75272227
O	N	-1.43651059	-4.16531504	-1.79389069
H	Y	-3.77365485	-4.28661301	3.20589118
O	N	-2.97014659	3.62079364	2.07528018
Si	Y	0.0390251	-0.63598232	5.58401608
Si	Y	-3.99346425	0.25194994	-5.47162767
Si	N	-1.18490748	0.43048969	3.0323473
Si	N	-2.73109713	-0.7980431	-2.92708556
Si	Y	-4.02174209	-0.66790228	3.98502069
Si	Y	-5.61454638	-1.78037401	-1.96601106
Al	N	-3.13578021	1.80662946	-1.13347924
Al	N	-0.87928837	-2.21131964	1.26031156
Si	Y	-6.00179919	0.76912145	-0.18331201
Si	Y	-2.27596732	-5.37133561	-1.02814987
Si	Y	-3.72964818	-3.25198684	2.23430777
Si	Y	-4.59759213	3.92677409	2.12007698
Si	N	-1.64554584	2.90063395	1.50404411
Si	N	-0.74062483	-2.71436646	-1.91298029
Si	Y	-3.69043532	4.39075655	-2.81311301
H	Y	-4.14045576	1.6636894	-5.51435624

H	Y	-3.57970558	-0.21958455	-6.7455468

Table S7 – Coordinates for DFT Model of α-MeOH (BEA)

element	constrained during optimization?	X	Y	Z
Fe	N	-0.87493352	0.20179363	-0.30248982
O	N	-1.03191452	-0.4772009	1.65429081
O	N	-2.40134985	0.23750702	-1.69300219
O	N	-1.94130703	1.95823977	0.18720259
O	N	-0.74770353	-1.87526633	-0.50682239
O	N	0.88647998	1.29258603	-0.2116378
H	N	0.7508182	2.23251501	-0.01363312
C	N	2.11106502	0.81270246	0.40400945
H	N	2.01810547	0.83468201	1.4896733
H	N	2.24989768	-0.21056128	0.06425877
H	N	2.94548428	1.42954035	0.07201882
O	Y	4.86222375	-4.50175858	0.32392216
O	Y	1.32971847	5.73640801	0.63172018
O	Y	6.92661469	-2.8718311	0.17822878
O	Y	6.08579872	4.35746043	0.02695722
O	Y	3.76264124	5.50804845	-0.35169763
O	Y	7.18619915	2.16889832	-0.92086971
O	Y	7.55170103	-0.40095558	-0.492804
Si	Y	3.306199	-4.91570932	0.27049828
Si	Y	-0.26963826	5.54440954	0.66203665
Si	Y	5.97546997	-3.86943969	-0.65168013
Si	Y	7.34137065	3.35935241	0.14788813
Si	Y	2.43899864	6.4211711	-0.31322922
Si	Y	7.60890536	0.76874804	-1.59714859
Si	Y	8.12160551	-1.7969487	0.07063202
Si	Y	5.25554136	5.34645529	-0.93821387
O	Y	2.56189504	-4.37672721	1.59205232
Si	Y	1.18790051	-4.27182016	2.42556286
H	Y	0.72859132	0.20943266	6.47990083
O	Y	2.62201567	-4.27056499	-1.03420526
H	Y	-0.80904953	5.83231922	-0.61957338
H	Y	7.40355231	2.81949879	1.45979321
H	Y	2.99663863	-3.26664594	-3.26862207
H	Y	8.6908364	-1.59671944	1.35604583
H	Y	8.52868543	4.09499349	-0.10809451

H	Y	5.32642561	-3.14332613	-1.68506719
H	Y	1.92443889	6.52544955	-1.63259697
H	Y	6.75215575	-4.90730955	-1.23131897
H	Y	2.76530904	7.70911782	0.18787637
H	Y	9.11922062	-2.29211991	-0.81025859
H	Y	8.93009145	0.88025818	-2.10552191
H	Y	5.20229524	4.79801204	-2.24693992
H	Y	6.70921423	0.46618623	-2.6532706
H	Y	5.88745552	6.6172627	-0.98444351
Si	Y	2.01968775	-3.94117256	-2.48948461
O	N	-0.00089567	0.06494848	4.08122606
O	N	-2.81945973	-0.05036195	-4.35043728
H	Y	0.80496602	-1.84626599	5.40973451
H	Y	3.20297956	-6.3308725	0.21315631
H	Y	-4.16176378	4.20178235	-4.14217424
H	Y	1.48142568	-4.1648645	3.81065218
H	Y	-2.55616521	5.29346766	-2.87447259
H	Y	-1.23473192	-0.95863924	6.07326066
H	Y	-5.23358062	-0.34357713	-5.12574895
H	Y	-3.94492642	-1.19254959	5.29166388
H	Y	-6.60568631	-1.55287148	-2.96575053
H	Y	1.65139022	-5.14860652	-3.13974833
H	Y	-0.83049217	6.42336406	1.62601567
O	N	0.7879022	-2.87591182	-2.39889864
O	N	-0.46387488	3.9495379	1.01747896
O	N	-0.92837877	1.9827154	2.62847584
O	N	-1.49288076	-1.8472495	-3.046787
O	N	-2.64027773	0.22864479	3.69694634
O	N	-4.12051997	-1.61724204	-2.63423801
H	Y	-5.11552461	0.2284386	3.87300752
H	Y	-5.74053094	-3.08185358	-1.44395163
O	Y	-4.16229468	-1.84316883	2.91101804
H	Y	-4.76631146	5.17121964	2.78178777
O	Y	-5.81294805	-0.6988504	-0.77939325
H	Y	-2.11054033	-6.61786718	-1.69632964
O	N	-4.69905515	1.70915586	-0.51457936
H	Y	-1.77300292	-5.47574493	0.28597019
O	N	-2.2635486	-3.16825164	1.58748661
H	Y	-4.98765599	4.07017779	0.76025552
O	N	-2.95892751	2.98532139	-2.35889162
H	Y	0.40597332	-5.43477486	2.19609087
O	N	0.51797619	-2.86705513	1.97282015
H	Y	-4.66701242	4.9129428	-1.99387416

H	Y	-6.13332053	0.72195437	1.2222701
H	Y	-3.70014072	-5.10205129	-0.95914543
H	Y	-4.63924355	-3.54587142	1.17859409
H	Y	-5.27940224	2.9120235	2.75459196
H	Y	-7.13453902	1.39752784	-0.75675988
O	N	-1.45064962	-4.19282593	-1.79828309
H	Y	-3.79002911	-4.27516369	3.20894152
O	N	-2.90919754	3.68290215	2.08169025
Si	Y	0.05698504	-0.64999457	5.57066695
Si	Y	-3.99010269	0.24404654	-5.4791496
Si	N	-1.17313151	0.41859019	3.02599014
Si	N	-2.73957246	-0.80994169	-2.92774361
Si	Y	-4.00707782	-0.65267736	3.97974768
Si	Y	-5.62071743	-1.76651353	-1.96541337
Al	N	-3.12104493	1.80439445	-1.15446412
Al	N	-0.88205328	-2.22483776	1.25468125
Si	Y	-5.98364296	0.79035701	-0.18816623
Si	Y	-2.30964666	-5.38229307	-1.02538609
Si	Y	-3.73952608	-3.2432827	2.23475796
Si	Y	-4.54918199	3.9420183	2.10476289
Si	N	-1.62855547	2.90557653	1.48493314
Si	N	-0.74804548	-2.74124449	-1.91014412
Si	Y	-3.64808201	4.38666151	-2.83131772
H	Y	-4.12567267	1.65682999	-5.52502483
H	Y	-3.58273207	-0.2339239	-6.75272911

Table S8 – Coordinates for DFT Model of MeOH-Lattice Complex (BEA)

element	constrained during optimization?	X	Y	Z
O	N	-1.06942049	-0.66917138	1.77002981
O	N	-2.32789161	0.30915243	-1.75601242
O	N	-1.9133366	2.05713545	0.21464748
O	N	-0.86053165	-2.16769033	-0.36864897
O	N	0.07851261	0.68211435	-1.07646296
H	N	-0.2223849	1.16237376	-0.28533347
C	N	0.82140306	1.56988289	-1.9275306
H	N	1.70434428	1.93669941	-1.40094447
H	N	1.13441994	0.98656233	-2.79144607
H	N	0.20725948	2.413284	-2.25485835
O	Y	4.84905553	-4.49380269	0.33423381

O	Y	1.33777062	5.74865296	0.72827339
O	Y	6.91775098	-2.86717533	0.21521131
O	Y	6.09371241	4.36516371	0.13301002
O	Y	3.77501161	5.52478289	-0.24540725
O	Y	7.19393641	2.18381215	-0.83149995
O	Y	7.55162155	-0.39106187	-0.42768271
Si	Y	3.29239766	-4.90366671	0.26894236
Si	Y	-0.26228637	5.55982543	0.74871516
Si	Y	5.96851447	-3.85418166	-0.62942921
Si	Y	7.34645673	3.36304141	0.25000871
Si	Y	2.45321697	6.44049882	-0.20419216
Si	Y	7.61687805	0.78961982	-1.51983261
Si	Y	8.11563814	-1.79396995	0.12438773
Si	Y	5.27043227	5.36574856	-0.82617283
O	Y	2.5427636	-4.3764491	1.59221663
Si	Y	1.16490037	-4.27674899	2.41995591
H	Y	0.69546102	0.164236	6.51717682
O	Y	2.61613724	-4.24386776	-1.03252268
H	Y	-0.79456742	5.8621718	-0.53247421
H	Y	7.40095383	2.80980624	1.55666988
H	Y	3.00401137	-3.21823708	-3.25478717
H	Y	8.678947	-1.60804238	1.4145508
H	Y	8.53664997	4.09854164	0.00733556
H	Y	5.32619944	-3.11618472	-1.6585937
H	Y	1.94542464	6.55925016	-1.52497393
H	Y	6.74575588	-4.88789335	-1.21571587
H	Y	2.77990171	7.72253622	0.3115098
H	Y	9.11649869	-2.28246547	-0.75654943
H	Y	8.94080698	0.90327194	-2.02054028
H	Y	5.22244444	4.83069219	-2.14063165
H	Y	6.72175293	0.49979472	-2.58338012
H	Y	5.90538182	6.63552366	-0.85642199
Si	Y	2.02153652	-3.89819838	-2.48715379
O	N	-0.01725854	0.02791329	4.11523276
O	N	-2.77133179	-0.05197932	-4.38182566
H	Y	0.77259692	-1.88071258	5.42667972
H	Y	3.18633682	-6.31794915	0.1967795
H	Y	-4.13342236	4.27492205	-4.08789035
H	Y	1.45183864	-4.18453976	3.80750018
H	Y	-2.5316979	5.35004184	-2.80125968
H	Y	-1.26837986	-0.99521543	6.08910221
H	Y	-5.2104524	-0.25785138	-5.12274607
H	Y	-3.97520068	-1.21502377	5.2918271

H	Y	-6.5958668	-1.48587541	-2.98185917
H	Y	1.65401278	-5.09831255	-3.151615
H	Y	-0.82574024	6.43047721	1.71885457
O	N	0.78540851	-2.84617173	-2.34855394
O	N	-0.48467331	4.01314419	1.20067597
O	N	-0.92347128	1.89886918	2.62247829
O	N	-1.45639825	-1.80531318	-2.96803884
O	N	-2.65618388	0.20116204	3.71963311
O	N	-4.10397122	-1.54290768	-2.62050849
H	Y	-5.13560581	0.22286032	3.88190977
H	Y	-5.7416357	-3.03209968	-1.47139736
O	Y	-4.18223947	-1.841084	2.90365093
H	Y	-4.77003602	5.17559813	2.84249622
O	Y	-5.81204316	-0.65577754	-0.78304167
H	Y	-2.11829404	-6.57356055	-1.74167605
O	N	-4.67210696	1.69592304	-0.51714954
H	Y	-1.78804991	-5.45237509	0.25375146
O	N	-2.22009021	-3.11570472	1.66059436
H	Y	-4.98389019	4.09561301	0.80885788
O	N	-2.97106471	3.01232318	-2.33461117
H	Y	0.38154096	-5.43561705	2.1749009
O	N	0.37668121	-2.9111599	1.92353512
H	Y	-4.64771362	4.96539136	-1.93498546
H	Y	-6.1391818	0.74544393	1.23128303
H	Y	-3.70817917	-5.06174698	-0.99704588
H	Y	-4.65439432	-3.52507389	1.15175566
H	Y	-5.28803663	2.91800685	2.78993176
H	Y	-7.12911807	1.44325147	-0.74572426
O	N	-1.46711115	-4.23114509	-1.93635162
H	Y	-3.81684499	-4.27679627	3.17877762
O	N	-2.92806895	3.62990408	2.19240348
Si	Y	0.02644828	-0.68442846	5.59575011
Si	Y	-3.96380939	0.33051562	-5.46378732
Si	N	-1.18130503	0.36045416	3.044126
Si	N	-2.71420393	-0.79830674	-2.95971316
Si	Y	-4.02960777	-0.6618972	3.98499767
Si	Y	-5.61631346	-1.71170838	-1.9787642
Si	N	-0.92610165	-2.20475243	1.25617743
Si	Y	-5.98246284	0.82779082	-0.17764699
Si	Y	-2.31794849	-5.34426264	-1.05911882
Si	Y	-3.75927739	-3.23533471	2.21537142
Si	Y	-4.55227438	3.95270909	2.1539684
Si	N	-1.61959664	2.91149279	1.54826463

Si	N	-0.75132602	-2.77806397	-1.86848614
Si	Y	-3.6257276	4.44527522	-2.77274006
H	Y	-4.09617182	1.7439631	-5.49627357
H	Y	-3.55134862	-0.13552178	-6.74033631
H	N	-1.31549439	0.3412137	-1.52681502
Al	N	-3.06823854	1.87640144	-1.06777356

Table S9 – Coordinates for DFT Model of α-OH···CH_3 Complex (CHA)

element	constrained during optimization?	X	Y	Z
Fe	N	0.43956566	0.0002841	0.76787327
O	N	-0.07750667	1.5082483	-0.56037765
O	N	1.65230782	1.69061476	1.20644832
O	N	1.65103493	-1.69017097	1.20759459
O	N	-0.07860585	-1.50806352	-0.55923202
O	N	-0.80588079	0.0013323	1.99839168
H	N	-1.78985265	0.00333617	2.02433995
C	N	-3.63709433	0.00033431	1.51924325
H	N	-3.62152262	0.9302752	0.96785195
H	N	-3.6190251	-0.93042656	0.96930704
H	N	-4.01060369	0.00046853	2.53496541
O	N	-1.73231354	0.00064424	-1.9567264
O	N	-2.33307251	2.43309357	-1.80977368
O	N	-2.3336837	-2.4309627	-1.81074441
O	Y	-4.18054375	3.3137707	-0.17803865
O	Y	-6.0538145	2.43860121	1.44080375
O	Y	-4.17956345	-3.31324777	-0.17943522
O	Y	-7.01118632	0.0001211	1.26158047
O	Y	-6.05294263	-2.43941297	1.44006774
Si	N	-1.06841561	1.46863281	-1.89096819
Si	N	-1.06840732	-1.46732644	-1.89049771
Si	Y	-5.23680809	3.73949866	0.95855558
Si	Y	-3.1226263	-3.73898055	-1.31677176
Si	Y	-7.39841183	1.55121008	1.43477609
Si	Y	-5.23582919	-3.73952417	0.95682368
Si	Y	-7.39771442	-1.55279845	1.43468822
Si	Y	-3.12434191	3.74004679	-1.31571904
O	N	-0.22681486	1.81614298	-3.22097441
O	N	-0.22662535	-1.81620306	-3.21996429
O	N	3.19485237	0.00014075	2.3221407

O	Y	4.14166443	2.00923425	-1.64948624
H	Y	3.83698812	4.24410954	-2.67062225
H	Y	6.26699869	2.33299077	-0.42169885
O	Y	2.33246753	2.46505917	-3.50165081
Si	Y	3.11647452	3.09742839	-2.2458615
Si	Y	5.08140669	1.55199829	-0.42600713
O	N	0.09971126	4.26530763	0.67898206
H	Y	-3.81518242	4.29692816	-2.42410969
H	Y	-0.81761429	6.65542972	0.35126662
O	N	2.06370024	3.49435729	-1.09318275
H	Y	-1.84910778	5.1012945	1.73051037
Al	N	0.94474648	2.9201839	0.06385808
Si	Y	-1.15939967	5.28562628	0.50349914
O	Y	5.46796142	-0.00008637	-0.59846492
O	N	3.24273918	-2.26555687	3.42919496
O	N	4.33162293	-1.95115203	0.98857863
Si	N	3.1102897	-1.56558141	1.97736212
O	Y	4.03602589	0.00020144	4.96026169
O	N	3.24318938	2.26596966	3.42885979
H	Y	4.64269909	-2.35812501	5.40889016
H	Y	4.64354027	2.35889088	5.40680012
O	N	4.33286587	1.95111559	0.98870666
H	Y	2.42491625	-1.73561078	5.6900006
H	Y	2.42538171	1.73740142	5.68917386
Si	N	3.11111482	1.56585638	1.97710364
Si	Y	3.59270897	-1.54593665	4.90484147
Si	Y	3.59345449	1.54707435	4.90487576
O	Y	1.58614901	-0.00103234	-4.014346
H	Y	0.86992122	-1.91231743	-5.41578259
H	Y	0.8702113	1.9106962	-5.41604299
Si	Y	1.1427779	-1.54618426	-4.07120145
Si	Y	1.14281952	1.54484465	-4.07184476
O	Y	4.14107955	-2.01078895	-1.64981393
H	Y	6.26670976	-2.33402304	-0.42035806
H	Y	3.83564198	-4.24592113	-2.66968921
O	Y	2.33287438	-2.46795453	-3.50021219
Si	Y	5.08069599	-1.55301136	-0.42604104
Si	Y	3.11507257	-3.09859301	-2.24452489
O	N	0.0984241	-4.26536378	0.68228785
H	Y	-0.81885808	-6.6546178	0.35358918
O	N	2.06265166	-3.49417041	-1.09093424
H	Y	-1.8510646	-5.09974246	1.73290616
Al	N	0.94310497	-2.9205198	0.0657613

Si	Y	-1.16114676	-5.28541994	0.50534586
O	Y	-2.09901942	4.82783747	-0.72027317
H	Y	-4.54664011	4.29661639	2.06719894
H	Y	-6.14287562	4.69904133	0.43413274
O	Y	-2.09610832	-4.82619466	-0.72184799
H	Y	-8.22785097	1.9557549	0.35575404
H	Y	-3.8134613	-4.29609679	-2.42468826
H	Y	-8.0883219	1.73589162	2.66234083
H	Y	-4.54431648	-4.29740709	2.06449057
H	Y	-8.22726273	-1.9572567	0.35531552
H	Y	-6.14135111	-4.69998669	0.43180572
H	Y	-8.08742606	-1.73811782	2.6616992

Table S10 – Coordinates for DFT Model of α-Fe(II) (CHA)

element	constrained during optimization?	X	Y	Z
Fe	N	0.64406224	0.00033164	0.57190717
O	N	-0.1741793	1.54244769	-0.49332666
O	N	1.5833205	1.7365958	1.25685225
O	N	1.58211543	-1.73628717	1.25798601
O	N	-0.17558635	-1.54210711	-0.491994
O	N	-1.82055954	0.00076919	-1.86089377
O	N	-2.44211283	2.43854763	-1.73589861
O	N	-2.44294202	-2.43622434	-1.73739881
O	Y	-4.25891576	3.31370039	-0.05283248
O	Y	-6.10765882	2.43867248	1.5939389
O	Y	-4.25788521	-3.31308683	-0.05428291
O	Y	-7.06761418	0.00020727	1.4289581
O	Y	-6.10686145	-2.43934992	1.59303196
Si	N	-1.17906326	1.47741305	-1.81405041
Si	N	-1.17921507	-1.47590045	-1.81353535
Si	Y	-5.29777071	3.73960074	1.09972273
Si	Y	-3.2179759	-3.73888301	-1.20717828
Si	Y	-7.4521883	1.55129565	1.60796747
Si	Y	-5.29703992	-3.73945335	1.09763089
Si	Y	-7.4515391	-1.552713	1.60776216
Si	Y	-3.21956249	3.74020812	-1.20592878
O	N	-0.34595561	1.81704696	-3.15185385
O	N	-0.34559619	-1.81708101	-3.15057835
O	N	3.06160646	0.00000761	2.33298365

O	Y	4.04057187	2.00922092	-1.64816452
H	Y	3.72074716	4.24416724	-2.6645497
H	Y	6.18399063	2.33296942	-0.45224735
O	Y	2.20393909	2.4651931	-3.47308869
Si	Y	3.00661261	3.09749241	-2.22910073
Si	Y	4.99853158	1.55201814	-0.43879751
O	N	0.04917566	4.29158107	0.75605052
H	Y	-3.92693426	4.29713982	-2.30382574
H	Y	-0.88820594	6.65545681	0.42656573
O	N	1.9768986	3.50044893	-1.0598991
H	Y	-1.89903472	5.1012751	1.82097761
Al	N	0.86144738	2.95032763	0.10852293
Si	Y	-1.22766356	5.28561286	0.58388588
O	Y	5.38242801	-0.00011681	-0.61714707
O	N	3.22388779	-2.26723277	3.44535878
O	N	4.26944492	-1.92135877	0.99410986
Si	N	3.05124339	-1.57434908	1.9975059
O	Y	4.03364769	-0.0000048	4.96230672
O	N	3.22424626	2.26734017	3.44509671
H	Y	4.64679844	-2.35838428	5.40182903
H	Y	4.64768074	2.35869081	5.39989145
O	N	4.27079749	1.92105162	0.99441378
H	Y	2.43349366	-1.73577045	5.71601527
H	Y	2.43399753	1.73715338	5.7152985
Si	N	3.05202538	1.57433414	1.99725408
Si	Y	3.58939779	-1.54621417	4.9135192
Si	Y	3.59017997	1.54701222	4.91359842
O	Y	1.45002969	-0.0008941	-3.97465119
H	Y	0.71296019	-1.91210126	-5.36534501
H	Y	0.71329482	1.91089582	-5.3654736
Si	Y	1.00576646	-1.5460708	-4.02501555
Si	Y	1.00594547	1.54506331	-4.02557401
O	Y	4.03990549	-2.01072906	-1.64860179
H	Y	6.18364375	-2.33411062	-0.45105658
H	Y	3.71927552	-4.24586527	-2.66386872
O	Y	2.2043244	-2.46781921	-3.47183123
Si	Y	4.99773177	-1.55311287	-0.4389192
Si	Y	3.00513203	-3.09849458	-2.22791028
O	N	0.04772027	-4.2916266	0.7590511
H	Y	-0.8896193	-6.65458944	0.42843848
O	N	1.97559335	-3.49999323	-1.05792076
H	Y	-1.90112295	-5.09975803	1.8230454
Al	N	0.85964675	-2.95058105	0.11034779

Si	Y	-1.22959475	-5.28536285	0.58533141
O	Y	-2.18545062	4.82786775	-0.62580867
H	Y	-4.591252	4.29660756	2.19787181
H	Y	-6.2116639	4.69915972	0.58881468
O	Y	-2.18273224	-4.82611979	-0.62781563
H	Y	-8.29763156	1.95589007	0.54145779
H	Y	-3.92533381	-4.29593019	-2.30475856
H	Y	-8.12370042	1.73594482	2.84569772
H	Y	-4.58910102	-4.29737421	2.19482383
H	Y	-8.297109	-1.95712064	0.54087571
H	Y	-6.21031968	-4.69989681	0.58613888
H	Y	-8.1228668	-1.73806457	2.84492296

Table S11 – Coordinates for DFT Model of α-O (CHA)

element	constrained during optimization?	X	Y	Z
Fe	N	0.43069028	0.00031886	0.72569816
O	N	-0.13936506	1.49426365	-0.53051914
O	N	1.60373886	1.6709757	1.20775213
O	N	1.60240342	-1.67046946	1.20888027
O	N	-0.14055575	-1.49399071	-0.52934538
O	N	-0.6598037	0.00118572	1.87604154
O	N	-1.82178329	0.00074995	-1.91635687
O	N	-2.40530669	2.44332665	-1.76025299
O	N	-2.40654389	-2.44049535	-1.7606462
O	Y	-4.24212824	3.31364969	-0.09477907
O	Y	-6.09492253	2.43865857	1.54744319
O	Y	-4.24105294	-3.31313233	-0.09603779
O	Y	-7.05417896	-0.00015129	1.38019583
O	Y	-6.09410797	-2.4390012	1.54692632
Si	N	-1.16003798	1.46593573	-1.85044767
Si	N	-1.1601781	-1.46449959	-1.84995349
Si	Y	-5.28380669	3.73957633	1.05521532
Si	Y	-3.19829467	-3.73894927	-1.24638447
Si	Y	-7.43943724	1.55127913	1.55823456
Si	Y	-5.2830515	-3.73947306	1.05329095
Si	Y	-7.43893225	-1.55274738	1.55794652
Si	Y	-3.19989665	3.74015868	-1.24536022
O	N	-0.31767842	1.81735801	-3.17732608
O	N	-0.31745724	-1.81802411	-3.17602851

O	N	3.17537792	0.00011283	2.31436653
O	Y	4.06131253	2.00917673	-1.66948803
H	Y	3.74399434	4.24408046	-2.68672864
H	Y	6.20176151	2.33294504	-0.46828316
O	Y	2.22921788	2.46505909	-3.49897936
Si	Y	3.02874439	3.09740264	-2.2529818
Si	Y	5.0162315	1.55201948	-0.4577567
O	N	0.0500761	4.26278177	0.71374154
H	Y	-3.90455485	4.29704353	-2.34494818
H	Y	-0.87261314	6.65543199	0.39288027
O	N	1.99169668	3.48626302	-1.08306239
H	Y	-1.8868873	5.10129862	1.78483981
Al	N	0.88080233	2.92167817	0.08283123
Si	Y	-1.21255552	5.2856853	0.5493707
O	Y	5.40061351	-0.00014354	-0.63510668
O	N	3.21470574	-2.26463463	3.41918341
O	N	4.27659146	-1.95552058	0.96279915
Si	N	3.07530149	-1.56316318	1.97067217
O	Y	4.03804343	0.00011604	4.94097824
O	N	3.21512233	2.26498882	3.41891261
H	Y	4.65009486	-2.35824801	5.38209029
H	Y	4.65096755	2.35881196	5.38002761
O	N	4.27801746	1.95531642	0.96303523
H	Y	2.43601659	-1.73564611	5.69078182
H	Y	2.43651637	1.7372912	5.68998594
Si	N	3.07618905	1.56339895	1.97045485
Si	Y	3.59389473	-1.54609549	4.89115305
Si	Y	3.59467998	1.54707782	4.8912114
O	Y	1.47654726	-0.00102546	-4.00230897
H	Y	0.74293639	-1.91227049	-5.39480732
H	Y	0.74325444	1.91071775	-5.39503773
Si	Y	1.03240811	-1.54622184	-4.05380105
Si	Y	1.03259938	1.54490917	-4.05445237
O	Y	4.06066809	-2.01079272	-1.66983524
H	Y	6.20143199	-2.33412153	-0.46697489
H	Y	3.74256234	-4.24594378	-2.68583889
O	Y	2.22960569	-2.46793012	-3.49758602
Si	Y	5.01547763	-1.55314182	-0.45781499
Si	Y	3.0273083	-3.09860802	-2.25168097
O	N	0.04889539	-4.26297057	0.71672264
H	Y	-0.87398071	-6.65461462	0.39511822
O	N	1.9905508	-3.48596408	-1.08088935
H	Y	-1.88893248	-5.09974758	1.78717579

Al	N	0.87908462	-2.92188439	0.08470401
Si	Y	-1.21434559	-5.2854378	0.55111969
O	Y	-2.16725299	4.82782146	-0.66262729
H	Y	-4.58002337	4.29661521	2.1550853
H	Y	-6.19644624	4.6991181	0.54201001
O	Y	-2.16449843	-4.8261883	-0.66436555
H	Y	-8.28224859	1.95584834	0.48953983
H	Y	-3.90292949	-4.29604772	-2.34564158
H	Y	-8.11408236	1.73595032	2.79421543
H	Y	-4.57783815	-4.29737352	2.15227522
H	Y	-8.28172147	-1.95716435	0.4890667
H	Y	-6.19505371	-4.69992237	0.53955113
H	Y	-8.11326769	-1.73810005	2.79350853

Table S12 – Coordinates for DFT Model of α-OH (CHA)

element	constrained during optimization?	X	Y	Z
Fe	N	0.37108239	-0.00136969	0.78271673
O	N	-0.1451366	1.49590057	-0.5267685
O	N	1.60550984	1.68319114	1.21096759
O	N	1.59896882	-1.67209074	1.21752678
O	N	-0.13953104	-1.50258828	-0.5339549
O	N	-0.85245754	0.00673157	2.05031402
H	N	-1.68753407	0.4239811	2.27662958
O	N	-1.80965153	-0.00407613	-1.92283604
O	N	-2.39679947	2.43482158	-1.76966602
O	N	-2.39973166	-2.44142114	-1.77416873
O	Y	-4.23316298	3.31256021	-0.11719167
O	Y	-6.08900955	2.43985486	1.52261509
O	Y	-4.2318172	-3.3140232	-0.10901817
O	Y	-7.04835097	0.00117932	1.35702122
O	Y	-6.08791643	-2.43798803	1.52896034
Si	N	-1.14446634	1.4606543	-1.85924787
Si	N	-1.14470447	-1.47125831	-1.85739416
Si	Y	-5.2772334	3.74023119	1.02994616
Si	Y	-3.18678772	-3.7415049	-1.25665747
Si	Y	-7.43364455	1.5525947	1.53199289
Si	Y	-5.27581895	-3.73889067	1.03921367
Si	Y	-7.43271452	-1.55159569	1.53650669
Si	Y	-3.18878097	3.7373718	-1.26645921

O	N	-0.30227872	1.8113666	-3.18649742
O	N	-0.30687104	-1.81924996	-3.18897912
O	N	3.17564456	0.00462808	2.31289952
O	Y	4.07327558	2.00638631	-1.67422905
H	Y	3.75778388	4.23979264	-2.69538526
H	Y	6.21145339	2.33204404	-0.46939892
O	Y	2.24468268	2.45947339	-3.50792981
Si	Y	3.04191143	3.09371058	-2.26142128
Si	Y	5.02597735	1.55101325	-0.460054
O	N	0.05016614	4.2556444	0.69944347
H	Y	-3.89131494	4.29277715	-2.36834982
H	Y	-0.86484284	6.6553587	0.37183142
O	N	1.99802742	3.48562136	-1.09766966
H	Y	-1.88167093	5.10320931	1.76413874
Al	N	0.8926704	2.91509517	0.07169203
Si	Y	-1.20487568	5.28570626	0.52965024
O	Y	5.41068153	-0.00132255	-0.6343889
O	N	3.22163368	-2.25868	3.41880993
O	N	4.27980869	-1.95044263	0.96274697
Si	N	3.07397369	-1.55943076	1.96792236
O	Y	4.03739963	0.0070397	4.9392173
O	N	3.22157568	2.27074245	3.41298265
H	Y	4.64889818	-2.35061252	5.38482572
H	Y	4.6494808	2.36640271	5.37583701
O	N	4.28470296	1.95532537	0.95834876
H	Y	2.4341667	-1.7277631	5.68836523
H	Y	2.43445089	1.74524416	5.68246379
Si	N	3.07780423	1.56739243	1.96343859
Si	Y	3.59364454	-1.53919442	4.89065437
Si	Y	3.59423579	1.55380967	4.88616878
O	Y	1.49313847	-0.007389	-4.00917242
H	Y	0.76224085	-1.92074291	-5.40014106
H	Y	0.76236906	1.90226747	-5.40599085
Si	Y	1.04928967	-1.55259056	-4.05897762
Si	Y	1.04916619	1.53834997	-4.06413262
O	Y	4.07290993	-2.01358756	-1.66869602
H	Y	6.2114137	-2.33497251	-0.46123849
H	Y	3.75688059	-4.25023576	-2.6820467
O	Y	2.2453266	-2.47358962	-3.49929891
Si	Y	5.02542138	-1.55401462	-0.45554881
Si	Y	3.04082462	-3.10230439	-2.25101869
O	N	0.05744847	-4.26454685	0.70875652
H	Y	-0.86538835	-6.65467246	0.39360064

O	N	2.0017943	-3.48684483	-1.08141634
H	Y	-1.88308587	-5.09781865	1.78145987
Al	N	0.88800745	-2.91720668	0.08201174
Si	Y	-1.20608343	-5.285223	0.54695913
O	Y	-2.15736912	4.82615035	-0.68344626
H	Y	-4.57546293	4.29888513	2.13042127
H	Y	-6.18881667	4.69891497	0.5136357
O	Y	-2.15400467	-4.82787244	-0.67094649
H	Y	-8.27439576	1.95542022	0.46125454
H	Y	-3.88920432	-4.3004099	-2.35636383
H	Y	-8.11050655	1.73893235	2.76658767
H	Y	-4.57273461	-4.29501994	2.14025755
H	Y	-8.27362877	-1.95755013	0.46653259
H	Y	-6.18683347	-4.70013763	0.52502926
H	Y	-8.10946788	-1.73504266	2.7709989

Table S13 – Coordinates for DFT Model of α-OCH_3 (CHA)

element	constrained during optimization?	X	Y	Z
Fe	N	-0.39157967	-0.0003875	0.75576297
O	N	0.09947851	-1.5110778	-0.5677878
O	N	-1.61634215	-1.69106569	1.21642237
O	N	-1.61517574	1.6903601	1.21769784
O	N	0.10075862	1.51116116	-0.56634329
O	N	0.94520129	-0.0014753	1.89644267
C	N	2.33594573	-0.00419693	2.09969198
H	N	2.78384044	-0.89340365	1.64419161
H	N	2.78602544	0.88769297	1.65164778
H	N	2.53954111	-0.00893839	3.17376884
O	N	1.74963488	-0.00044584	-1.96505294
O	N	2.35123354	-2.4359787	-1.82069557
O	N	2.35199852	2.43429448	-1.82172653
O	Y	4.19614853	-3.31345979	-0.17773241
O	Y	6.06746241	-2.43854465	1.44340497
O	Y	4.19489531	3.31332604	-0.17847148
O	Y	7.02497059	-0.00003192	1.26541803
O	Y	6.06650571	2.43947779	1.44302098
Si	N	1.08998464	-1.46970346	-1.89974815
Si	N	1.09010923	1.46883043	-1.89900081
Si	Y	5.25085583	-3.73944682	0.96030104

Si	Y	3.13914275	3.73919333	-1.31682263
Si	Y	7.41203057	-1.55112686	1.43892822
Si	Y	5.24986663	3.73960742	0.95900827
Si	Y	7.41128512	1.55288178	1.4390576
Si	Y	3.14094508	-3.73990437	-1.31641232
O	N	0.24503359	-1.81806302	-3.22674805
O	N	0.24473046	1.81886671	-3.22525606
O	N	-3.16277284	-0.00032706	2.32506694
O	Y	-4.12468104	-2.0090964	-1.65798
H	Y	-3.8188483	-4.24390658	-2.67892157
H	Y	-6.25132907	-2.33299658	-0.4325227
O	Y	-2.31343359	-2.46478932	-3.50818121
Si	Y	-3.09878881	-3.09726109	-2.25325323
Si	Y	-5.06573322	-1.55202208	-0.43545763
O	N	-0.08456613	-4.26432298	0.6768569
H	Y	3.83308265	-4.2966777	-2.42402107
H	Y	0.83249554	-6.65537204	0.3478833
O	N	-2.04947209	-3.48934168	-1.09536325
H	Y	1.86246355	-5.10131653	1.72835561
Al	N	-0.92635005	-2.91868596	0.05880871
Si	Y	1.17413042	-5.28562889	0.50059915
O	Y	-5.45216056	0.00011334	-0.60820649
O	N	-3.22956227	2.26580714	3.42227758
O	N	-4.3030539	1.94177438	0.9761366
Si	N	-3.08409964	1.56390408	1.97139573
O	Y	-4.02633868	-0.00054451	4.95202876
O	N	-3.22991189	-2.26676285	3.4216664
H	Y	-4.63344743	2.35777079	5.40017921
H	Y	-4.63422117	-2.35929041	5.3977542
O	N	-4.30425748	-1.94193527	0.97602388
H	Y	-2.41597842	1.73522149	5.6836502
H	Y	-2.41639605	-1.73774848	5.68258889
Si	N	-3.08487338	-1.564499	1.97095617
Si	Y	-3.58293668	1.54560596	4.89719398
Si	Y	-3.58363651	-1.54740451	4.89703341
O	Y	-1.56660499	0.0013647	-4.01985207
H	Y	-0.84889654	1.9127397	-5.42041707
H	Y	-0.84911244	-1.91025088	-5.42094206
Si	Y	-1.1231067	1.54657736	-4.07620059
Si	Y	-1.12322979	-1.54454474	-4.0770828
O	Y	-4.1241428	2.01088727	-1.6580169
H	Y	-6.25110919	2.33404061	-0.43085277
H	Y	-3.81763185	4.24611893	-2.67738473

O	Y	-2.31393687	2.46821225	-3.50639308
Si	Y	-5.06506726	1.55308285	-0.43528666
Si	Y	-3.09750582	3.09879499	-2.25149456
O	N	-0.08344757	4.26437308	0.68081576
H	Y	0.83354104	6.65467781	0.35114515
O	N	-2.04841058	3.48927507	-1.09272723
H	Y	1.86426802	5.09972466	1.73146489
Al	N	-0.92472537	2.91904748	0.06108231
Si	Y	1.17565545	5.28549073	0.50316538
O	Y	2.11501817	-4.82764453	-0.72211862
H	Y	4.55961002	-4.29659069	2.06805959
H	Y	6.15762305	-4.69892356	0.43670116
O	Y	2.11197689	4.8263639	-0.72308104
H	Y	8.24265354	-1.95558314	0.36078422
H	Y	3.83122436	4.29639473	-2.4240245
H	Y	8.10060389	-1.73588418	2.66723255
H	Y	4.5571583	4.29739128	2.0659434
H	Y	8.24200519	1.9574276	0.36062
H	Y	6.15595894	4.70013315	0.43503042
H	Y	8.09965503	1.73812525	2.66683391

Table S14 – Coordinates for DFT Model of C-O Recombination TS (CHA)

element	constrained during optimization?	X	Y	Z
Fe	N	0.43565724	-0.00320197	0.76391618
O	N	-0.08792594	1.51364167	-0.55221599
O	N	1.64433117	1.71136807	1.20969844
O	N	1.64308036	-1.69431003	1.20980373
O	N	-0.0904309	-1.52586141	-0.55274544
O	N	-0.79950884	0.00616413	2.03935795
H	N	-1.43131338	0.62815474	2.41497695
C	N	-3.4693545	0.01551726	1.40781789
H	N	-3.53364874	0.93770336	0.84802883
H	N	-3.31298448	-0.91419027	0.88328304
H	N	-3.81846821	-0.01375737	2.43116477
O	N	-1.72983373	-0.00588261	-1.95690732
O	N	-2.33759234	2.42797791	-1.81176791
O	N	-2.34287733	-2.4368044	-1.81439792
O	Y	-4.18356632	3.31146662	-0.18045778
O	Y	-6.05477374	2.43949421	1.44239032

O	Y	-4.18120077	-3.31529555	-0.16787733
O	Y	-7.01187123	0.00046932	1.26928913
O	Y	-6.05300179	-2.43851824	1.45181352
Si	N	-1.07230425	1.46293424	-1.88892608
Si	N	-1.07376498	-1.47777861	-1.88518612
Si	Y	-5.23838667	3.73955945	0.95667608
Si	Y	-3.12535555	-3.74326559	-1.30535084
Si	Y	-7.39919337	1.55184475	1.43967318
Si	Y	-5.2361435	-3.73948167	0.97042397
Si	Y	-7.39792927	-1.55215673	1.44604275
Si	Y	-3.12839453	3.73577736	-1.31996863
O	N	-0.22696936	1.81258038	-3.21645174
O	N	-0.23010841	-1.82519059	-3.21493894
O	N	3.16951652	0.00714733	2.32349412
O	Y	4.13748644	2.00552964	-1.65792968
H	Y	3.83130168	4.2382231	-2.68337618
H	Y	6.26407467	2.3322238	-0.4330929
O	Y	2.32621054	2.45718591	-3.50909056
Si	Y	3.11142242	3.09227573	-2.2554194
Si	Y	5.07860144	1.55101419	-0.43448551
O	N	0.09429443	4.26354975	0.67875462
H	Y	-3.82062721	4.29021418	-2.42873172
H	Y	-0.82049055	6.65498515	0.33848544
O	N	2.05962301	3.49701188	-1.10432796
H	Y	-1.85022245	5.10353882	1.72206329
Al	N	0.94309471	2.92466139	0.05369736
Si	Y	-1.16191407	5.28548529	0.49393581
O	Y	5.465266	-0.00135669	-0.60417041
O	N	3.24492842	-2.25683625	3.43018871
O	N	4.32722841	-1.9372267	0.98952852
Si	N	3.10206192	-1.56011566	1.97722832
O	Y	4.03930905	0.01023947	4.9560954
O	N	3.24405841	2.27493435	3.42260381
H	Y	4.64688885	-2.34704051	5.40898292
H	Y	4.64686793	2.36996089	5.39707331
O	N	4.3285036	1.94515702	0.98117492
H	Y	2.42929617	-1.72434506	5.69117669
H	Y	2.42912836	1.74866241	5.68312637
Si	N	3.10439592	1.5724478	1.97177581
Si	Y	3.5962138	-1.53608839	4.90437996
Si	Y	3.5963863	1.5569062	4.8979766
O	Y	1.57979829	-0.01011692	-4.01582209
H	Y	0.86243068	-1.92443007	-5.4125436

H	Y	0.86200647	1.89856125	-5.42075436
Si	Y	1.13655215	-1.555497	-4.0690478
Si	Y	1.13617005	1.5355727	-4.07614446
O	Y	4.13762943	-2.0144826	-1.64988627
H	Y	6.26463719	-2.33477614	-0.42204633
H	Y	3.83150735	-4.25178771	-2.66478136
O	Y	2.327539	-2.47579904	-3.49738556
Si	Y	5.07848332	-1.55399367	-0.42806672
Si	Y	3.11119942	-3.10371881	-2.24124171
O	N	0.10612091	-4.2768663	0.69189583
H	Y	-0.81931388	-6.65502987	0.36850593
O	N	2.06286453	-3.49823504	-1.08471023
H	Y	-1.85031582	-5.09747253	1.7456843
Al	N	0.93819312	-2.92830206	0.06884865
Si	Y	-1.16165942	-5.28558749	0.51774885
O	Y	-2.10268066	4.82488789	-0.72786734
H	Y	-4.54724376	4.29904436	2.06333462
H	Y	-6.14529428	4.69782971	0.43114176
O	Y	-2.09804686	-4.82909907	-0.709408
H	Y	-8.22986433	1.9539942	0.36070349
H	Y	-3.81734455	-4.30282688	-2.41145138
H	Y	-8.08782051	1.73895637	2.66759105
H	Y	-4.54335543	-4.29492361	2.07849601
H	Y	-8.22856234	-1.95900878	0.36840591
H	Y	-6.14205947	-4.70121001	0.44836827
H	Y	-8.08629113	-1.73504699	2.67417724

Table S15 – Coordinates for DFT Model of α-MeOH (CHA)

element	constrained during optimization?	X	Y	Z
Fe	N	-0.49667952	0.03250597	0.65651902
O	N	0.09353453	-1.51370229	-0.61056201
O	N	-1.59339729	-1.88715759	1.24640659
O	N	-1.58890051	1.75946508	1.24777801
O	N	0.14723964	1.62012919	-0.54861354
O	N	0.51954987	-0.56940842	2.3508367
H	N	0.18999296	-1.42172011	2.66300371
C	N	1.90854677	-0.36253709	2.69093041
H	N	2.54408865	-1.06400162	2.14800576
H	N	2.15119483	0.65611169	2.39816213

H	N	2.04473782	-0.47316586	3.76686606
O	N	1.73889873	0.05651086	-1.94569605
O	N	2.3608952	-2.38152177	-1.87714608
O	N	2.39615066	2.48524307	-1.8256888
O	Y	4.21150022	-3.29468697	-0.26377078
O	Y	6.08218179	-2.45409008	1.37614615
O	Y	4.20978814	3.33063902	-0.12454975
O	Y	7.03958245	-0.01230287	1.2500415
O	Y	6.08088414	2.42285197	1.47878947
Si	N	1.089499	-1.41936196	-1.93157416
Si	N	1.11158347	1.54249125	-1.88378305
Si	Y	5.26583819	-3.74455009	0.86538278
Si	Y	3.15440369	3.780386	-1.25402093
Si	Y	7.42668942	-1.56669192	1.39088947
Si	Y	5.26432647	3.73286327	1.0220537
Si	Y	7.42572695	1.53662131	1.45657721
Si	Y	3.15672677	-3.69705271	-1.41157623
O	N	0.26265208	-1.7316995	-3.28199234
O	N	0.26642805	1.89545612	-3.21253624
O	N	-2.99392807	-0.05806929	2.29400018
O	Y	-4.10886846	-1.9598649	-1.7190703
H	Y	-3.80254474	-4.17259989	-2.78689748
H	Y	-6.23594276	-2.30972929	-0.5015389
O	Y	-2.29696508	-2.37626687	-3.57785955
Si	Y	-3.08271657	-3.0351385	-2.33684521
Si	Y	-5.05046643	-1.52880157	-0.487492
O	N	-0.07163567	-4.28435304	0.58401164
H	Y	3.84929744	-4.23026428	-2.53045498
H	Y	0.84789712	-6.64716603	0.18995122
O	N	-2.03716239	-3.48438253	-1.20034107
H	Y	1.87726824	-5.1225487	1.60330227
Al	N	-0.92118596	-2.94309064	-0.02875452
Si	Y	1.18937801	-5.28092006	0.371682
O	Y	-5.43689464	0.02663846	-0.62767843
O	N	-3.23159663	2.1887346	3.44720544
O	N	-4.28772097	1.8719938	1.00957354
Si	N	-3.04192384	1.52335497	1.9836168
O	Y	-4.01304341	-0.09136673	4.93187033
O	N	-3.25741854	-2.33793306	3.36573874
H	Y	-4.62045494	2.25691578	5.42955744
H	Y	-4.62089623	-2.45904042	5.32750767
O	N	-4.2979403	-1.90748509	0.92758178
H	Y	-2.4030515	1.62863556	5.70060086

H	Y	-2.40322473	-1.8434943	5.62618695
Si	N	-3.0551116	-1.62881502	1.9247309
Si	Y	-3.56967515	1.45571249	4.90991735
Si	Y	-3.57016841	-1.63679214	4.84441691
O	Y	-1.55012598	0.1001865	-4.03707121
H	Y	-0.83205514	2.04076112	-5.39669405
H	Y	-0.83200527	-1.78136627	-5.47796324
Si	Y	-1.10672211	1.64626795	-4.06060586
Si	Y	-1.10662731	-1.44414405	-4.12677709
O	Y	-4.10861244	2.05920938	-1.63420261
H	Y	-6.23604844	2.3562664	-0.40129725
H	Y	-3.80192249	4.3154997	-2.60604426
O	Y	-2.29781245	2.55559056	-3.47188606
Si	Y	-5.05001638	1.57565187	-0.42173455
Si	Y	-3.08186234	3.15946265	-2.20421844
O	N	-0.09204641	4.30718976	0.76981544
H	Y	0.84800948	6.65984586	0.47432851
O	N	-2.04080813	3.55301797	-1.04343385
H	Y	1.87835899	5.07615283	1.82186557
Al	N	-0.90819473	2.97623614	0.0965137
Si	Y	1.19017294	5.28776905	0.59752054
O	Y	2.13066974	-4.79716569	-0.84075523
H	Y	4.57423927	-4.32500913	1.96088313
H	Y	6.17285647	-4.69269713	0.32195719
O	Y	2.12694716	4.85470321	-0.63782208
H	Y	8.25772138	-1.94823531	0.30473809
H	Y	3.84683623	4.3608912	-2.34896789
H	Y	8.11484252	-1.77730809	2.61526147
H	Y	4.57118703	4.26710063	2.14027751
H	Y	8.25679977	1.96390627	0.38721906
H	Y	6.17053582	4.70429787	0.51880209
H	Y	8.11365097	1.69593537	2.68823671

Table S16 – Coordinates for DFT Model of CH_3 Radical Escape TS (CHA)

element	constrained during optimization?	X	Y	Z
Fe	N	-0.42325988	-0.00001559	0.78301668
O	N	0.07037008	-1.49955078	-0.53626773
O	N	-1.66192762	-1.67371466	1.22678969
O	N	-1.66221319	1.67350103	1.22673924

O	N	0.07005806	1.49909166	-0.53660963
O	N	0.8872166	0.00070105	1.96682918
H	N	1.84940885	0.00087394	1.9371646
C	N	4.38574851	-0.04093813	-0.46803989
H	N	4.61381279	-0.75214552	0.3066797
H	N	4.16423679	-0.38627711	-1.46488546
H	N	4.43038397	1.01579209	-0.26634365
O	N	1.69793385	-0.00068867	-1.98289992
O	N	2.34357013	-2.43048714	-1.74548294
O	N	2.343914	2.42826172	-1.74114246
O	Y	4.16960175	-3.31115635	-0.08555197
O	Y	6.01957309	-2.4344541	1.55976545
O	Y	4.16541055	3.31611505	-0.0880205
O	Y	6.9780231	0.00432698	1.39347318
O	Y	6.01617026	2.44343298	1.55785962
Si	N	1.07457348	-1.47817856	-1.86101801
Si	N	1.07463659	1.47662031	-1.86149577
Si	Y	5.20955258	-3.73594301	1.06672216
Si	Y	3.12459539	3.74092385	-1.2404936
Si	Y	7.36350878	-1.54654415	1.57241944
Si	Y	5.20529745	3.74314059	1.06282743
Si	Y	7.36133708	1.55746949	1.5716297
Si	Y	3.1297947	-3.7381368	-1.23752062
O	N	0.2489546	-1.86281098	-3.18906316
O	N	0.24785918	1.86295843	-3.18862078
O	N	-3.24748519	-0.00032465	2.3161802
O	Y	-4.13172738	-2.01081735	-1.6741517
H	Y	-3.81158911	-4.24576407	-2.69033982
H	Y	-6.27398918	-2.3352755	-0.47639148
O	Y	-2.29627935	-2.46627087	-3.50052881
Si	Y	-3.09769949	-3.09856576	-2.25576495
Si	Y	-5.08883481	-1.55370755	-0.4641359
O	N	-0.11919901	-4.2585798	0.71100524
H	Y	3.83636008	-4.29476267	-2.33597219
H	Y	0.80107032	-6.65415456	0.39747564
O	N	-2.06472869	-3.4864235	-1.08115543
H	Y	1.81226062	-5.09922015	1.79075532
Al	N	-0.95670559	-2.91408118	0.08596859
Si	Y	1.14001836	-5.28410806	0.55418852
O	Y	-5.47363452	-0.00185857	-0.64244171
O	N	-3.30005928	2.26499538	3.41487771
O	N	-4.34412082	1.95012297	0.95315026
Si	N	-3.14350899	1.5620349	1.96622435

O	Y	-4.12026126	-0.00017032	4.9359731
O	N	-3.2985142	-2.26539289	3.4156819
H	Y	-4.73431837	2.35796849	5.37541546
H	Y	-4.73289237	-2.35904104	5.37444448
O	N	-4.34370828	-1.95202246	0.95433226
H	Y	-2.52042522	1.73658368	5.68792352
H	Y	-2.51923399	-1.73642779	5.68792479
Si	N	-3.14299342	-1.56278966	1.96682164
Si	Y	-3.6769556	1.54617279	4.88640902
Si	Y	-3.67623731	-1.54684666	4.88717972
O	Y	-1.54405785	0.00013917	-4.00343507
H	Y	-0.80896327	1.91147916	-5.39484378
H	Y	-0.80746682	-1.91160745	-5.39419586
Si	Y	-1.10076688	1.54527937	-4.05401131
Si	Y	-1.09933316	-1.54533413	-4.05384995
O	Y	-4.13305028	2.00926031	-1.67544292
H	Y	-6.2759356	2.33173517	-0.47616462
H	Y	-3.81428863	4.24427116	-2.69143234
O	Y	-2.29901189	2.46697693	-3.50027951
Si	Y	-5.08960942	1.5512809	-0.46491275
Si	Y	-3.09927452	3.09730103	-2.25590695
O	N	-0.12105639	4.25934637	0.71117871
H	Y	0.79596258	6.6558964	0.39662469
O	N	-2.06664039	3.48524595	-1.08085844
H	Y	1.80933575	5.10184518	1.79074072
Al	N	-0.95733947	2.913915	0.0855779
Si	Y	1.13671906	5.2868504	0.55351477
O	Y	2.0965486	-4.82617665	-0.65637376
H	Y	4.5043855	-4.29320744	2.16522974
H	Y	6.12377153	-4.69509793	0.55490139
O	Y	2.08912112	4.82782558	-0.66025741
H	Y	8.20827114	-1.95093689	0.50535064
H	Y	3.83061606	4.29807312	-2.33859526
H	Y	8.03611645	-1.73060238	2.80968944
H	Y	4.4980411	4.30090263	2.16044671
H	Y	8.20583571	1.96207292	0.5039673
H	Y	6.11782802	4.70373314	0.55033667
H	Y	8.03358444	1.74340341	2.80820261

Table S17 – Coordinates for DFT Model of MeOH-lattice complex (BEA)

element	constrained during optimization?	X	Y	Z
O	N	0.23875467	-1.90385893	-0.51721361
O	N	-1.5198645	-2.21068051	1.45656972
O	N	-1.73065459	2.40695958	1.35224349
O	N	0.07406308	1.99968837	-0.5115548
O	N	0.67012203	-1.12027788	2.05485961
H	N	0.90450173	-1.07159549	1.11086445
C	N	0.95515199	0.10677302	2.7376365
H	N	0.40101404	0.93995993	2.30247832
H	N	0.65668452	-0.03159447	3.77577931
H	N	2.02747897	0.31018569	2.7022753
O	N	1.51961619	0.05592869	-1.62331749
O	N	2.45987781	-2.35198205	-1.93358611
O	N	2.36411832	2.46481477	-1.82512686
O	Y	4.22915551	-3.27591937	-0.21362643
O	Y	6.0964446	-2.4054383	1.41452962
O	Y	4.17450178	3.35017582	-0.13469453
O	Y	7.03393322	0.04269235	1.26415211
O	Y	6.0561786	2.47206994	1.47279119
Si	N	1.0892969	-1.50158883	-1.82660282
Si	N	1.02391303	1.57578114	-1.78341679
Si	Y	5.28943811	-3.70700174	0.91728411
Si	Y	3.11319502	3.78110576	-1.2659976
Si	Y	7.43380664	-1.50719474	1.41830679
Si	Y	5.22818577	3.77127705	1.00590243
Si	Y	7.4080491	1.59647973	1.45575486
Si	Y	3.17530681	-3.69719017	-1.35551653
O	N	0.26091687	-1.70512518	-3.21352424
O	N	0.21916682	1.83384097	-3.16743072
O	N	-2.56433286	0.02387973	2.02492867
O	Y	-4.10469942	-2.02117826	-1.66317382
H	Y	-3.78275988	-4.2410113	-2.71144282
H	Y	-6.22629729	-2.37696199	-0.43789189
O	Y	-2.29330312	-2.43997288	-3.52194237
Si	Y	-3.0710556	-3.0937501	-2.27317183
Si	Y	-5.0469567	-1.5864338	-0.43355791
O	N	-0.17691352	-4.5231512	0.66988404
H	Y	3.86981072	-4.23499799	-2.47092361
H	Y	0.89345936	-6.65094065	0.27775559
O	N	-2.09802868	-3.56244945	-1.09604557

H	Y	1.91360767	-5.10541414	1.67499915
Si	Y	1.22426799	-5.28012351	0.44635398
O	Y	-5.44646508	-0.03550315	-0.58683867
O	N	-3.29714147	2.09980697	3.4469828
O	N	-4.31584489	1.76826999	1.03490861
Si	N	-2.99008699	1.59534208	1.94924238
O	Y	-4.01014734	-0.09138108	4.96999909
O	N	-3.28935471	-2.16909323	3.37432725
H	Y	-4.63524649	2.25641369	5.44789401
H	Y	-4.59800537	-2.46017036	5.38876518
O	N	-4.19880959	-1.84135853	0.95378636
H	Y	-2.41232223	1.64844772	5.71989027
H	Y	-2.38475639	-1.82419115	5.67707486
Si	N	-2.96605004	-1.54127409	1.93314276
Si	Y	-3.57907835	1.4588349	4.93350774
Si	Y	-3.55485396	-1.63386663	4.89609485
O	Y	-1.56736635	0.03813303	-4.0054817
H	Y	-0.86774075	1.97191918	-5.38405116
H	Y	-0.83716278	-1.85066583	-5.43053885
Si	Y	-1.13644996	1.58742508	-4.04372889
Si	Y	-1.11161208	-1.50339116	-4.08181594
O	Y	-4.13655611	1.99843278	-1.6148696
H	Y	-6.26370404	2.28962734	-0.38013403
H	Y	-3.84997813	4.24812845	-2.60784358
O	Y	-2.33356268	2.49254027	-3.46086232
Si	Y	-5.07142104	1.51840698	-0.39608516
Si	Y	-3.11979169	3.10157753	-2.19702625
O	N	-0.24274896	4.41509503	0.64135128
H	Y	0.78736313	6.65765559	0.44106939
O	N	-2.05663759	3.55213682	-1.03672211
H	Y	1.83319845	5.09462406	1.80074402
Si	N	-0.98050381	3.09324406	0.08905518
Si	Y	1.14073013	5.28950495	0.57598897
O	Y	2.15922116	-4.80022698	-0.77250045
H	Y	4.60479882	-4.28297412	2.01950834
H	Y	6.20291051	-4.65276467	0.38056317
O	Y	2.07850708	4.85279502	-0.6573162
H	Y	8.26561914	-1.89195121	0.33388733
H	Y	3.79868734	4.35716721	-2.36762779
H	Y	8.12617099	-1.70111838	2.64306214
H	Y	4.53309132	4.31011366	2.12071506
H	Y	8.23343945	2.02064593	0.38076733
H	Y	6.12550395	4.74531503	0.49189284

H	Y	8.09722727	1.77252501	2.68443015
H	N	-0.69475622	-1.73610267	1.86640164
Al	N	-0.88050228	-3.1437323	0.0021482

Supplementary References

34. Schmidt, J. E.; Deimund, M. A.; Xie, D.; Davis, M. E. Synthesis of RTH-Type Zeolites Using a Diverse Library of Imidazolium Cations. *Chem. Mater.* **27**, 3756–3762 (2015).

35. Hallaert, S. D.; Bols, M. L.; Vanelderen, P.; Schoonheydt, R. A.; Sels, B. F.; Pierloot, K. Identification of α-Fe in High-Silica Zeolites on the Basis of Ab Initio Electronic Structure Calculations. *Inorg. Chem.* **56**, 10681–10690 (2017).

36. Frisch, M. J.; Trucks, G. W.; Schlegel, H. B.; Scuseria, G. E.; Robb, M. A.; Cheeseman, J. R.; Scalmani, G.; Barone, V.; Mennucci, B.; Petersson, G. A.; et al. Gaussian09. Gaussian, Inc.: Wallingford, CT 2009.

37. Baerlocher, C.; McCusker, L. B. http://www.iza-structure.org/databases/ (accessed Feb 4, 2018).

38. Grimme, S.; Antony, J.; Ehrlich, S.; Krieg, H. A Consistent and Accurate Ab Initio Parametrization of Density Functional Dispersion Correction (DFT-D) for the 94 Elements H-Pu. *J. Chem. Phys.* **132**, 154104 (2010).